

# Accurate localization and coactivation profiles of the FEF and IFJ: an ALE and MACM fMRI meta-analysis

Marco Bedini<sup>1\*</sup>, Emanuele Olivetti<sup>1,2</sup>, Paolo Avesani<sup>1,2</sup> & Daniel Baldauf<sup>1</sup>

1. Center for Mind/Brain Sciences (CIMEC), University of Trento, Trento, Italy

2. NeuroInformatics Laboratory (NILab), Bruno Kessler Foundation (FBK), Trento, Italy

\* Corresponding author at: Center for Mind/Brain Sciences, University of Trento

via delle Regole, 101, 38123, Trento (TN), Italy

Phone: +39 0461 282753

E-mail: [marco.bedini@unitn.it](mailto:marco.bedini@unitn.it)

## Abstract

The frontal eye field (FEF) and the inferior frontal junction (IFJ) are prefrontal structures involved in mediating multiple aspects of goal-driven behavior. Despite being recognized as prominent nodes of the networks underlying spatial attention and oculomotor control, and working memory and cognitive control, respectively, the limited quantitative evidence on their precise localization has considerably impeded the detailed understanding of their structure and connectivity. In this study, we performed an activation likelihood estimation (ALE) fMRI meta-analysis selecting studies that employed standard paradigms to accurately infer the localization of these regions in stereotaxic space. For FEF, we found the highest spatial convergence of activations for prosaccades and antisaccades contrasted against a fixation baseline at the junction of the precentral sulcus with the superior frontal sulcus. For IFJ, we found consistent activations across oddball/cueing, working memory, Stroop and task-switching paradigms at the junction of the precentral sulcus with the inferior frontal sulcus. We related these clusters to previous meta-analyses, sulcal/gyral neuroanatomy and a recent comprehensive brain parcellation, highlighting important differences compared with their results and taxonomy. Finally, we employed the peak coordinates of these clusters as seeds to perform a meta-analytic connectivity modeling (MACM) analysis, which revealed systematic coactivation patterns spanning the frontal, parietal and temporal cortices. We then decoded the behavioral domains associated with the coactivation patterns of each seed, suggesting that these may allow FEF and IFJ to support their respective specialized roles in flexible behavior. Our study provides meta-analytic groundwork for investigating the relationship between functional specialization and connectivity of two crucial structures within the prefrontal cortex.

**Keywords:** Prefrontal Cortex, Visual Attention, Saccadic Eye Movements, Working memory, Activation Likelihood Estimation, Meta-analytic Connectivity Modeling

## Introduction

Owing to the capabilities that likely derive from the massive expansion in the cortical surface allowed by the folding patterns of the cortex (Van Essen 2007; Welker 1990; Zilles et al. 2013), which particularly affected the prefrontal and association cortices (Donahue et al. 2018; Toro et al. 2008), humans possess one of the most complex behavioral repertoires observed in nature (Mesulam 1998; Miller and Cohen 2001). A fundamental aspect of functional specialization in the human brain is its relationship with cortical neuroanatomy (Van Essen 2007). Microstructural features pertaining to cortical architecture (i.e., cyto- and myelo-architecture), such as cell types and layer organization, are a major determinant of the functional organization of the brain, and they provide important information about regional segregation (Brodmann 1909; Amunts et al. 2020). Over the past 30 years, magnetic resonance imaging (MRI; and in particular, functional MRI) became the dominant technique for investigating this organization non-invasively and *in vivo* (Eickhoff et al. 2018). Although regional delineations as inferred based on architectonic criteria (e.g., cytoarchitecture) generally agree well with information gathered from MRI/fMRI (Amunts and Zilles 2015), such correspondences should be always interpreted with caution, as the former may be weak predictors of functional organization in highly heterogeneous regions, for example when regions sit at the boundary of different Brodmann areas (BA; Brodmann 1909). Moreover, this relationship may be affected by strong inter-individual differences, which were not taken into account in most of the previous invasive studies characterized by small sample sizes (Amunts and Zilles 2015). In addition to the previous prevalent invasive and lesion-based approaches, another way of conceptualizing functional organization and, more in general, the relationship between cognitive processes and their neural substrate, emerged from fMRI research with the functional localization approach (Kanwisher 2010). Specialized computations are performed by brain regions that can be reliably identified across individuals with fMRI using standard tasks (thus usually referred to as functional localizers; Kanwisher et al. 1997; Kanwisher 2010; O'Craven et al. 1999; Peelen and Downing 2005). In combination with the functional localization approach, research on structural MRI has shown that, despite the remarkable inter-individual variability in the organization of the gyri and sulci across the whole cortex (Desikan et al. 2006; Destrieux et al. 2010; Ono et al. 1990; Petrides 2019), these functional modules can also be localized on the basis of specific anatomical landmarks (Fischl et al. 2008), which suggests a developmental link between the functional differentiation of brain regions and the mechanisms of cortical maturation (Zilles et al. 2013).

In sum, in the human brain, functional specialization appears to be tightly linked and possibly follows from brain structure, although it remains to be established exactly to which degree this principle holds within specific systems. We have argued that in the prefrontal cortex (PFC), two structures, the frontal eye field (FEF) and the inferior frontal junction (IFJ), have largely overlapping but complementary roles, being involved in several orchestrating functions such as attention, working memory, cognitive control, and other top-down processes (Baldauf and Desimone 2014; Bedini and Baldauf 2021). While the FEF has been studied extensively both in human and non-human primates, its actual localization and relationship to sulcal morphology in humans, and correspondence to the macaque FEF has proven to be difficult to establish (Amiez and Petrides, 2009; Petit and Pouget 2019; Schall et al. 2020; Tehovnik et al. 2000; but see Koyama et al. 2004). Evidence also suggests that

FEF localization may be affected by substantial individual differences (Amiez et al. 2006; Kastner et al. 2007; Paus 1996; see Bedini and Baldauf 2021, for a discussion of this issue in the context of the multimodal parcellation (MMP1) by Glasser et al. (2016). Contrary to the prevailing view that the human FEF lies in the ventral bank of the superior precentral sulcus (sPCS), near its junction with the superior frontal sulcus (SFS; see Paus 1996 and Vernet et al. 2014, for a meta-analysis and a review of FEF localization, respectively), some authors have also argued that instead, a region localized ventrally in the dorsal branch of the inferior PCS (iPCS; for the detailed analysis of the morphology of the PCS see Germann et al. 2005), termed the inferior FEF (iFEF, or sometimes the lateral FEF) may better correspond to the functional profile of the putative homolog of the macaque FEF (Kastner et al. 2007; Schall et al. 2020). Moreover, it has been raised the related question of whether the inferior FEF has been under-reported in the fMRI literature (Derrfuss et al. 2012). In topographic mapping studies, peaks corresponding to the iFEF have been already reported (Kastner et al. 2007; Mackey et al. 2017) albeit they were not as consistent as FEF peaks in their presence across subjects and relative localization. Moreover, at least one study has previously reported activations in the iFEF using a saccadic localizer task, which were clearly segregated from those elicited by a Stroop task (Derrfuss et al. 2012). In the latter study, the analyses were performed in native space on an individual-subject basis, which is a very powerful approach that allows for carefully studying dissociations in adjacent neuroanatomical regions (Fedorenko 2021). The study by Frost and Goebel (2012) showed that, by leveraging the individual-subject approach and then improving the alignment in the cortical folding patterns (hence limiting the influence of the anatomical variability across subjects) using a technique termed curvature-driven cortex-based alignment, the overlap in FEF localization increased by 66.7% in the left hemisphere and 106.5% in the right hemisphere compared to volume-based registration in a sample of 10 subjects, suggesting that the FEFs are indeed strongly bound to a macro-anatomical location (i.e., the junction of the sPCS and the SFS; Paus 1996), and more generally the presence of a strong structure-to-function relationship in this region (see also Wang et al. 2015, described hereafter). The IFJ, a region found ventrally and anteriorly with respect to the iFEF, is typically localized near the junction of the iPCS with the IFS, sometimes encroaching into the caudal bank of the IFS (Derrfuss et al. 2005). The IFJ was only much more recently characterized as a separate brain region (based on structural; Amunts et al. 2006; and functional criteria; Brass et al. 2005) that performs both specialized (Baldauf and Desimone, 2014; Bedini and Baldauf 2021) and general domain computations (Assem et al. 2020; Derrfuss et al. 2005), in line with the multiple demand hypothesis (Duncan 2010). In the study by Derrfuss et al. (2009), 13 out of 14 subjects showed activations localized between the caudal bank of the IFS and the iPCS that corresponded to the anatomical description of the IFJ in a task-switching paradigm. Currently however, due to the interspersed and close arrangement of specialized and multiple demand regions near the IFJ, common activation foci resulting from various cognitive processes have not been reported yet across experiments (see however Assem et al. 2020, for evidence from high-quality fMRI data and improved inter-subject alignment methods; and Derrfuss et al. 2005, for meta-analytic evidence).

Clearly there is a need to better characterize the relationship between anatomy and functional specialization within the PFC. That such a link can in principle be successfully accomplished has been demonstrated in the visual system, where studies have shown that despite the inter-individual variability in the overall size, shape and position of the early visual cortex, specific anatomical landmarks (i.e., sulci) coincide very well with the

borders of primary visual areas as derived from various sources of data, including cytoarchitecture, retinotopic mapping, myelin content and resting-state fMRI functional connectivity (Abdollahi et al. 2014; Fischl et al. 2008; Glasser et al. 2016; Sereno et al. 1995). For example, in Hinds et al. (2008) the authors used surface-based registration methods (Fischl et al. 1999) to identify V1 in new subjects from cortical folding information (i.e., the stria of Gennari), and showed that these methods outperformed volumetric methods in labeling this structure (see also Hinds et al. 2009). Similarly, Benson et al. (2012) used folding information to predict visual responses within the striate cortex to a retinotopic mapping fMRI protocol. They first created a group-level reconstruction of the population receptive fields in V1 and used this information to fit their model to the anatomically defined V1 (Hinds et al. 2008) on a left-out subject and a second sample, reporting a prediction accuracy that matched the one derived from 10-25 min of fMRI retinotopic mapping. When moving up into the cortical visual hierarchy however, the relationships between cortical folding and other neuroanatomical information become more difficult to establish and interpret (Coalson et al. 2018; Glasser et al. 2016). Wang et al. (2015) created a probabilistic atlas of 25 topographic visual areas and showed that anatomical variability (as measured by the variance in gyral-sulcal convexity across subjects) and the overlap of functional activations (measured as a peak probability values) were negatively correlated, particularly in higher-order visual areas, suggesting that the former may play an important role in shaping functional organization. Similarly, in one of the most comprehensive efforts to parcel the cortical surface with high-resolution non-invasive methods, Glasser et al. (2016) found that the lateral prefrontal cortex (PFC) is one of the brain districts where the intrinsic neuroanatomical variability is higher than in the rest of the brain (Glasser et al. 2016; see also Juch et al. 2005), as measured by a decrease in the test-retest reliability of their parcellation. While the former limitations (i.e., the weaker association between cortical folding and function, and inter-individual variability, which particularly affects volumetric group-level analyses; Coalson et al. 2018) have posed significant challenges to the interpretation of the relationship between cortical folding and functional specialization in higher-order visual regions, some studies have shown that adopting an individual-level approach in defining sulci may bear important implications for understanding cognitive function within the PFC (Amiez et al. 2006; Amiez and Petrides 2018; Derrfuss et al. 2009; Miller et al. 2021). In particular, the recent study by Miller et al. (2021) provided evidence that tertiary sulcal morphology in the lateral PFC (which was manually defined on a subject-by-subject basis) is associated with an antero-posterior myelin gradient, distinct connectivity fingerprints, as well as multiple dissociable cognitive components, which highlight the functional relevance of these previously overlooked sulci. Taken together, these studies point to the need to better characterize the relationship between sulcal morphology and functional specialization within the PFC. This research line may in the future allow predicting functional activity from neuroanatomical information alone, thus accomplishing one of the fundamental goals of contemporary cognitive neuroscience in terms of inferring structure-to-function relationships (Felleman and Van Essen 1991; Osher et al. 2016; Passingham et al. 2002; Saygin et al. 2012; Young et al. 2000).

In summary, the organization of the regions localized along the banks of the major sulci of the posterior-lateral PFC (plPFC), namely the SFS, the sPCS, the iPCS, and the IFS, has yet to be clarified spatially. In particular, the exact localization of the FEF in standard space, and its relationship with the localization of the iFEF as inferred using saccadic localizer tasks, needs to be reassessed in the light of recent fMRI evidence (see Grosbras et al.



2005; Paus 1996 for previous meta-analyses using fMRI and PET experiments). Further, the exact localization of the IFJ in standard space and the convergence of activations across paradigms also needs to be re-examined (see Derrfuss et al. 2005, for convergence across task-switching and Stroop paradigms). These pieces of evidence would provide important clues on how to better interpret activations in the pPFC based on combined structural and functional criteria. Coordinate-based meta-analyses offer a convenient way to summarize and model the uncertainty in the activations found across several PET/fMRI experiments (Fox et al. 2014) based on specific paradigms and contrasts of interest, overcoming inter-individual variability and allowing to establish adequately powered brain-behavior relationship. The activation likelihood estimation (ALE) technique in particular allows inferring the spatial convergence of the foci reported in several independent fMRI experiments (Eickhoff et al. 2009, 2012). Here, we employed the ALE meta-analytic technique to accurately infer the localization of the FEF and IFJ activation peaks in standard space, thus aiming at resolving the discrepancies in the previous literature (in particular, concerning the precise localization of the FEF and IFJ). To do so, we analyzed data from standard functional localizers and paradigms (to partially overcome the issue of inter-individual variability in FEF localization), and we investigated the potential spatial overlap in the activations elicited by shared cognitive processes by analyzing data from several distinct paradigms that involve a common cognitive component (described more in detail in the “study selection criteria”). By using these peaks as seeds, we also performed a meta-analytic connectivity modeling (MACM) analysis (Robinson et al. 2010) to investigate the coactivation profiles of FEF and IFJ in fMRI studies across paradigms. Overall, our study aims to provide meta-analytic groundwork for investigating the relationship between functional specialization and connectivity of the FEF and IFJ in larger sample sizes compared to the typical ones used in neuroimaging studies (~20 subjects), as well as suggesting some consensus guidelines and anatomical priors to accurately localize these regions with fMRI and to guide future non-invasive brain stimulation studies.

## Materials and methods

### Activation likelihood estimation fMRI meta-analysis method

The activation likelihood estimation (ALE) is a very powerful meta-analytic technique that allows for assessing the spatial convergence of the activations reported in the neuroimaging literature (Eickhoff et al. 2009, 2012). As a coordinate-based technique, ALE takes as input the activation peaks reported by several independent neuroimaging studies (PET/fMRI) and tests their significance against a null distribution of the foci across the whole brain (Eickhoff et al. 2012). This ALE feature is particularly convenient given that in the neuroimaging literature results are usually reported and summarized as x, y, z coordinates in standard space (Talairach or MNI), rather than as full activation maps accompanied by a statistical summary of the effect sizes, and even more rarely shared in that form (for important initiatives in neuroimaging data sharing see however NeuroVault: <https://neurovault.org/>, Gorgolewski et al. 2015; OpenNeuro: <https://openneuro.org/>, Markiewicz et al. 2021; BALSA: <https://balsa.wustl.edu/>, Van Essen et al. 2017, and Anima: <https://anima.inm7.de/index.php>, Reid et al. 2015, among other initiatives). This becomes very relevant in the case of brain regions that may be under-reported in the literature (such as for example, the iFEF; Derrfuss et al. 2012; Kastner et al. 2007) or

which only recently began to be included in the brain atlases taxonomy (such as the IFJ; Bedini and Baldauf 2021; Sundermann and Pfliegerer 2012). Here, we exploit this feature of the ALE technique by applying it to analyze two independent collections of fMRI studies performed over the last 30 years with the primary aim of accurately inferring FEF and IFJ localization in MNI152 space using the GingerALE software (v. 3.0.2; <https://www.brainmap.org/ale/>). In the ALE procedure, each set of foci reported in a study is modeled as a three-dimensional Gaussian distribution centered around the coordinates and whose size is determined based on the experiment sample size (Eickhoff et al. 2009, 2012). In particular, larger sample sizes result in tighter Gaussians, which reflects lower uncertainty about the ‘true’ location reported, whereas lower samples lead to larger Gaussians that are more spread around the respective peak coordinates, thus conveniently reflecting lower confidence about their corresponding ‘true’ locations. These activations are then combined into a modeled activation map for each experiment of a study. Importantly, in the revised ALE algorithm, within-study effects that could result from the summation of adjacent foci are minimized, so that studies that reported activation in a higher number or more densely organized foci won’t drive the ALE results disproportionately (Turkeltaub et al. 2012). By computing the union of all these modeled activation maps, an ALE score for each voxel in the brain is obtained (Eickhoff et al. 2009, 2012). The significance of these scores is then assessed by comparing them with the null distribution obtained by randomly reassigning the modeled activations across the whole brain with a permutation approach. Finally, the thresholded p-values are usually corrected for multiple comparisons using either voxel-level or cluster-level FWE, as the use of uncorrected p-values and false discovery rate is generally unadvised since it can lead to spurious findings (Eickhoff et al. 2016).

As we introduced earlier, the present curated ALE meta-analysis focused on specific cognitive functions (described more in detail in the ‘Study selection criteria’) in which the FEF and IFJ and the associated brain networks are relatively well-known to be involved. More specifically, in what we will refer to here further as the ‘FEF sample’, we applied the ALE technique to several independent fMRI studies all requiring the planning and execution of visually-guided and voluntary eye movements, as a considerable number of previous studies clearly showed that these types of tasks elicit activation near the FEF, among other eye fields (for previous meta-analyses see Cieslik et al. 2016; Grosbras et al. 2005; Jamadar et al. 2013; Paus 1996). In particular, tasks requiring the execution of prosaccades and antisaccades contrasted against a fixation baseline are the most prevalent and consensually established approach to functionally localizing the FEF in the human fMRI literature (Amiez et al. 2006; Amiez and Petrides 2018). However, when studies are not only interested in localizing the FEF but other regions too, sometimes also covert spatial attention paradigms are employed, for example, to localize all the main nodes of the dorsal attention network (Corbetta and Shulman 2002). Therefore, studies employing adaptations of the spatial cueing paradigm (Posner et al. 1980) were included to check for their spatial agreement with the previous group as a control analysis. In the case of the ‘IFJ sample’, it is arguably more difficult to pinpoint a universally accepted functional localizer for this region, and in fact, very few studies have implemented a separate and targeted localizer paradigm to isolate the IFJ (for relevant examples see Baldauf and Desimone 2014; Zanto et al. 2010; Zhang et al. 2018) for subsequent second-level analyses. In addition, there is increasing evidence that the IFJ may be in fact characterized as a region more generally involved in different and often overlapping flexible cognitive operations (i.e., a ‘multiple demand’ region; Assem et al. 2020; Derrfuss et al. 2005; Sundermann and Pfliegerer 2012), which may even further complicate

the definition of a standard localization method. Therefore, in the ‘IFJ sample,’ we anticipate that we analyzed data from a more heterogeneous collection of fMRI studies investigating covert attention, working memory, and cognitive control across a wider range of paradigms. Whenever the sample sizes of the studies retrieved allowed for it, we also carried out post hoc control analyses to examine potential spatial discrepancies between the IFJ peaks derived from splitting up the full localizer sample according to specific cognitive functions and paradigms.

## Study selection criteria

The selection criteria of the sample of studies for the meta-analysis followed the best-practice recommendations and guidelines by Müller et al. (2018). Multiple bibliographic searches were performed between May 2019 and January 2021 (cutoff date). A final search was conducted with the same criteria and cutoff dates (i.e., 1st of January 1990 - 1st of January 2021) by the first author MB to comply with the updated PRISMA guidelines (Page et al. 2021) and as a sanity check. The selection procedure is reported in Figures 1 and 2 (created based on the PRISMA flow diagram; Page et al. 2021), which refer to the ‘FEF sample’ and the ‘IFJ sample’, respectively. All the bibliographical searches were carried out using Web of Science (<https://www.webofscience.com>). We searched records in the Web of Science Core Collection using the keywords ‘fMRI’ AND ‘frontal eye field’ (all fields) in the first instance, and ‘fMRI’ AND ‘inferior frontal junction’ (all fields) in the second. We complemented these results with other sources (Google Scholar, personal collection of articles and references cited by the studies retrieved) by one of the authors (MB). In the FEF sample, our search identified a total of 711, from which we removed all the review papers. 665 records were further screened, and 470 of these were sought for retrieval to assess their adequacy with respect to the inclusion criteria (described below). In the IFJ sample, 375 results were identified, from which, after removing review papers, 356 records were further screened, and 142 of these were sought for retrieval to assess their adequacy with respect to our original inclusion criteria. The general inclusion criteria consisted of the following. Each study selected: 1. Reported coordinates in standard space (either MNI or Talairach); 2. Was an fMRI study (no PET studies were included); 3. Performed on a scanner of 3T or higher field; 4. Tested and reported results from healthy adults (18-60; or an appropriate control group in the case of clinical studies); 5. The study acquired fMRI data with a FOV that was sufficiently large to cover the frontal cortex and in particular its posterior aspect. Even though the latter criterion would lead to the inclusion of studies with partial brain coverage, which is generally not recommended in ALE analyses (Müller et al. 2018), given that our main research question focused on the standard localization of FEF and IFJ, we motivate it by accepting the tradeoff derived from having access to a larger sample for these regions, as opposed to having less sensitivity in detecting other regions that are consistently active during the tasks included (which however are not the main focus of the present study), but not reported simply due to the lack of brain coverage. The last group of inclusion criteria are specific to each sample (the FEF or the IFJ) and are primarily related to the type of experimental paradigm utilized in the fMRI study and the specific contrasts analyzed (described more in detail below). Here, we strived to find a balance that would adequately represent the various localization methods that have been pursued in the fMRI literature, while also assigning a higher weight in the sample to the more standardized localization practices and well-validated approaches.

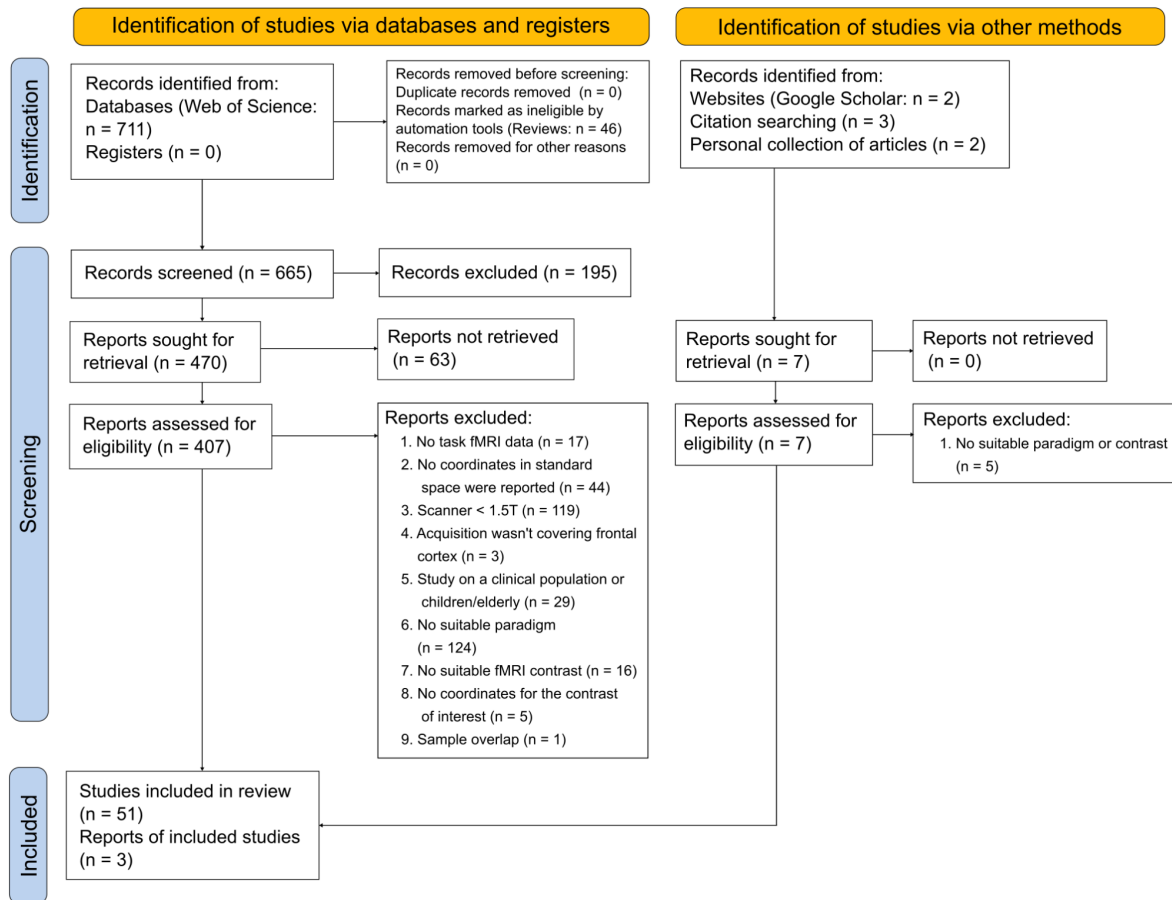


**Figure 1.** PRISMA2020 flow chart of the procedure that was carried out to select the studies included in the FEF sample.

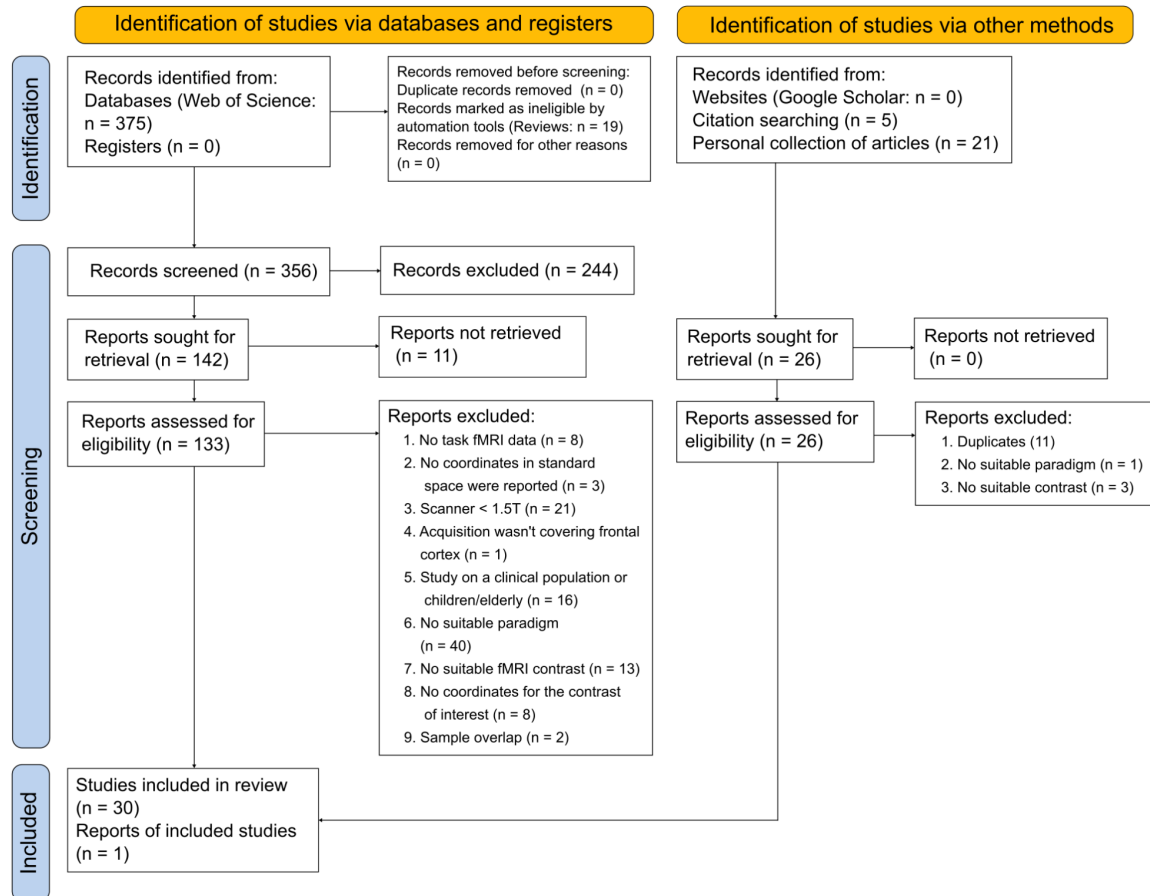


**Figure 2.** PRISMA2020 flow chart of the procedure that was carried out to select the studies included in the IFJ sample.

## FEF sample inclusion criteria

The human FEF is a well-characterized region in the fMRI literature (Bedini and Baldauf 2021), although some uncertainties persist regarding the correspondence of its localization obtained from fMRI compared with other methods (i.e., brain stimulation; Vernet et al. 2014) and with the macaque FEF (Koyama et al. 2004; Petit and Pouget 2019). The region is crucially involved in the top-down control of eye movements and spatial attention (Astafiev et al. 2003; Beauchamp et al. 2001; Corbetta et al. 1998), and it is considered a prominent node of the dorsal attention network (Corbetta and Shulman 2002; De Pasquale et al. 2010; Fox et al. 2006; Yeo et al. 2011). A very simple and time-efficient yet effective way to localize the FEF in fMRI scans is to have participants perform an experimental block of visually-guided saccades towards an unpredictable peripheral target, and contrast this activation with a fixation block (Amiez and Petrides 2006). The resulting activations - usually found near the junction of the SFS and the sPCS - are then assumed to correspond to the FEF (Paus 1996). However, depending on the statistical thresholds and analytical approach adopted, in addition to this superior cluster, often this type of contrast reveals a more widespread pattern of activity along the banks of the iPCS (Beauchamp et al. 2001; Kastner et al. 2007). Therefore, this localization method doesn't seem to have adequate functional specificity if not combined with the additional anatomical criteria mentioned above. Building on this approach, the antisaccade task and its neural mechanisms have been extensively studied in the primate

neurophysiology literature (Munoz and Everling 2004), and this task has been employed as a measure of inhibitory control in healthy and clinical populations in humans (Hutton and Ettinger 2006). Briefly, in the antisaccade task, the subject is required to keep fixation until a visual target appears and to look at its mirror location (Hallett 1978). Computationally, this requires at least two mechanisms: the first one inhibits a reflexive saccade towards the visual onset, and the second is responsible for executing a saccade towards the opposite location (the endpoint is in this case endogenously generated; Munoz and Everling 2004). An interesting feature of this task is that compared to the prosaccade task, it gives rise to frequent directional errors (that are often corrected with a subsequent saccade), which are assumed to reflect a failure to inhibit reflexive behavior (Hutton and Ettinger 2006; Munoz and Everling 2004; Pierrot-Deselleigny et al. 2002). Inserting a short (e.g., 200 ms) gap period before the presentation of the target decreases saccadic reaction times (Saslow 1967) and further increases the ratio of these directional errors (Munoz and Everling 2004). fMRI studies comparing the regions involved in prosaccade vs antisaccade task performance have found overlapping activations in the FEF in both tasks, although the antisaccade task recruits additional regions that seem to reflect the increased executive demands of this task (McDowell et al. 2008). Within FEF, there is also an increased activity (measured as a BOLD percent signal change) in the antisaccade compared to the prosaccade task, which is particularly evident during the preparatory phase (i.e., when the cue is being presented; Brown et al. 2006; Connolly et al. 2002; Curtis and Connolly 2004; Curtis and D'Esposito 2003; Ford et al. 2005) and when the two tasks are presented in a mixed fashion (Pierce and McDowell 2016, 2017). Based on these results, it could be hypothesized that contrasting antisaccades vs prosaccades may offer better specificity to localize clusters of activity within the FEF compared to the prosaccade vs fixation blocked design described earlier, which is the current gold standard (Amiez and Petrides 2018). Finally, in modified versions of the spatial cueing paradigm (Fan et al. 2005; Posner 1980), univariate analyses contrasting valid vs neutral/invalid trials are often used to localize all the main regions belonging to the dorsal attention network (Corbetta and Shulman 2002), which are subsequently used as ROIs for functional and effective connectivity analyses (for examples, see Vossel et al. 2012, and Wen et al. 2012). It can be argued that, even though these adaptations are not generally employed as independent functional localizers for the FEF, they may be well adept to isolate this region under the assumption that covert and overt shifts of spatial attention have a shared and overlapping source in this region, which seems well supported by fMRI (Astafiev et al. 2003; Beauchamp et al. 2001; Corbetta et al. 1998; Jerde et al. 2012) and comparative evidence (Buschman and Miller 2009; Moore and Fallah 2001; reviewed in Fiebelkorn and Kastner 2020). Indeed, the studies that directly investigated this question generally reported a strong degree of spatial overlap, although they also suggest that the signal measured in covert paradigms tends to be weaker than in overt tasks (Beauchamp et al. 2001; De Haan et al. 2008) and thus possibly less robust across fMRI data analysis pipelines (Botvinik-Nezer et al. 2020). Thus, an open question is whether prosaccades and covert spatial attention tasks are equally efficient in localizing the FEF.

In summary, for the reasons introduced above, we included in the FEF sample all the studies that investigated the planning and execution of visually-guided and voluntary eye movements (prosaccades and antisaccades) as well as covert spatial attention using both blocked and event-related designs, analyzing mainly the following contrasts: 1. prosaccades > fixation; 2. antisaccades > fixation; 3. prosaccades & antisaccades > fixation; 4. anti-saccades > pro-saccades; 5. valid > neutral/invalid trials (see Figure 1 for an overview of the selection



procedure following the PRISMA2020 guidelines; Page et al. 2021; for the full list of studies and the related information see Table 1 and Tables S1 and S2 in the Supplementary information). Combining these contrasts allowed us to carry out our main analysis complemented by three control analyses, respectively designed to replicate a previous study and to explore two additional research questions. In our main localizer analysis, we pooled together all studies that reported at least a contrast related to the planning and execution of prosaccades, both prosaccades and antisaccades, and antisaccades, contrasted with a fixation baseline. Our hypothesis was that the voxels where these activations converged more strongly (i.e., the peaks of the respective clusters, as indexed by the voxel with the highest ALE value) would provide accurate localization of the FEF in standard space (i.e., MNI152). In the first control analysis, we applied a less stringent multiple comparison correction method in order to reveal other consistently active peaks in neighboring frontal sites (see Activation likelihood estimation procedure for further details). The second control analysis was intended as a replication of the ALE meta-analysis by Cieslik et al. (2016), who performed an ALE contrast analysis to isolate the cluster/s uniquely involved in the antisaccade task by analyzing prosaccades > fixation vs antisaccades > prosaccades in two equal samples of 12 experiments (see also Jamadar et al. 2013, for previous results), although we did not explicitly carry out an ALE contrast analysis due to sample imbalance. Finally, the third control analysis was carried out to compare the topography and the sources of overt and covert attention near the putative FEF. For this analysis, we used prosaccades > fixation vs valid > neutral/invalid trials in covert spatial attention tasks, as we hypothesized that the inclusion of endogenous factors would make this comparison fairer in terms of the paradigm (considering that, strictly speaking, visually-guided saccades are a 100% ‘valid’ condition).

## **IFJ sample inclusion criteria**

In contrast to the FEF, the IFJ doesn't have a broadly accepted homolog in the macaque (Bedini and Baldauf 2021; see however Bichot et al. 2015, 2019; and Neubert et al. 2014) and its role started to be investigated only much more recently with fMRI (Brass et al. 2005). Its functional profile remains to date not well understood and is characterized by a remarkable functional heterogeneity (Muhle-Karbe et al. 2016; Ngo et al. 2019). Consistent with this idea, recent high-resolution fMRI studies showed that the IFJ (and in particular, the posterior IFJ as defined according to the MMP1 by Glasser et al. 2016) belongs to the core multiple-demand system of the brain (Assem et al. 2020, 2021), which identifies a set of regions that are engaged in multiple processes often across different cognitive domains (Duncan 2010). This particular position in the cognitive processing architecture arguably poses a severe challenge in trying to define a gold standard for an fMRI localization method for this region, which would allow to effectively segregate it from adjacent coactive regions (for an excellent example of such an approach see however Derrfuss et al. 2012; we return to this point in the discussion). Several promising approaches to localize the IFJ both at the individual and at the group level have nevertheless previously been reported from different research groups ranging from attention and working memory to cognitive control paradigms. For example, the series of studies from the group led by Brass and colleagues were critical in establishing the IFJ as a region involved in task preparation and more generally in cognitive control (Brass and Von Cramon, 2002, 2004; Derrfuss et al. 2004; see also Cole and Schneider 2007).

**Table 1.** List of the studies included in the FEF localizer sample

Study	N	Age	Paradigm	Contrast	Scanner	Design	Eye tracker	Results reported for	N° of foci	Multiple FEF foci	Software	Space
Alkhan et al. (2011)	8	26 ± 4	Functional localizer	Pro-saccades > Fixation	3T	Blocked	Y	Whole-brain	19	N	AFNI	Talairach
Amiez and Derriford (2018)	13	22.6 ± 2.8	Functional localizer	Pro-saccades > Fixation	3T	Blocked	N	FEF foci	2	N	SPM12b	MNI
Alm and Gilchrist (2013)	11	26.9-22-33	Functional localizer	Pro-saccades > Fixation	3T	Blocked	N	Whole-brain	24	Y	SPM8	MNI
Bir et al. (2016)	14	22-56	Functional localizer	Pro-saccades > Fixation	3T	Blocked	N	Whole-brain	12	N	Brain Voyager QX 1.10	Talairach
Bir et al. (2016)	14	22-56	Functional localizer	Anti-saccades > Fixation	3T	Blocked	N	Whole-brain	18	Y	Brain Voyager QX 1.10	Talairach
Bernham et al. (1999)	11	25.6 ± 7.1; 18-43	Functional localizer	Pro-saccades > Fixation	3T	Blocked	N	ROIs	14	Y	AFNI	Talairach
Braga et al. (2016)	20	26.2; 21-36	Functional localizer	Pro-saccades > Fixation	3T	Blocked	Y	Whole-brain	7	N	FSL	MNI
Brown et al. (2006)	10	26; 22-33	Functional localizer	Pro-saccades > Fixation	4T	<i>Event-related</i>	Y	Whole-brain	17	N	Brain Voyager 2000	Talairach
Brown et al. (2006)	10	26; 22-33	Functional localizer	Anti-saccades > Fixation	4T	<i>Event-related</i>	N	Whole-brain	21	N	Brain Voyager 2000	Talairach
Brown et al. (2006)	7	24.8 ± 3.2	Functional localizer	Pro-saccades > Fixation	4T	Blocked	N	Whole-brain	7	Y	Simulate	Talairach
Connolly et al. (2000)	7	24.8 ± 3.2	Functional localizer	Anti-saccades > Fixation	4T	Blocked	N	Whole-brain	13	Y	Simulate	Talairach
Connolly et al. (2002)	8	NA	Functional localizer	Pro-saccades > Fixation	4T	Blocked	N	ROIs	4	N	Simulate	Talairach
Connolly et al. (2005)	5	NA	Functional localizer	Pro-saccades > Fixation	4T	Blocked	N	ROIs	5	N	Simulate / Brain Voyager 4.9	Talairach
Connolly et al. (2007)	8	NA	Functional localizer	Pro-saccades > Fixation	4T	Blocked	N	ROIs	2	Y	Simulate / Brain Voyager 4.9 / QX	Talairach
Christophel et al. (2018)	22	24.4 ± 0.83	Functional localizer	Pro-saccades > Fixation	3T	<i>Event-related</i>	N	FEF foci	2	N	SPM8	MNI
Curtis & Connolly (2008)	12	21-35	Functional localizer	Pro-saccades & Anti-saccades > Fixation	3T	<i>Event-related</i>	Y	ROIs	32	Y	Caret	MNI
DesSouza et al. (2003)	10	26.6 ± 1.0	Functional localizer	Pro-saccades & Anti-saccades > Fixation	4T	Blocked	Y	Whole-brain	9	N	Brain Voyager 2000 4.4	Talairach
Dierker et al. (2013)	20	19-28	Functional localizer	Pro-saccades > Fixation	3T	Blocked	N	FEF foci	2	N	Brain Voyager QX 2.3	Talairach
Fernandez-Ruiz et al. (2018)	25	21.7 ± 1.9; 18-25	Functional localizer	Pro-saccades & Anti-saccades > Fixation	3T	<i>Event-related</i>	Y	Whole-brain	18	N	Brain Voyager QX 2.8.4	Talairach
Emanson et al. (2014)	24	26.7 ± 4.9	Functional localizer	Pro-saccades > Fixation	3T	Blocked	Y	Whole-brain	8	N	SPM8	MNI
Erkhan et al. (2016)	6	NA	Functional localizer	Pro-saccades & Anti-saccades > Fixation	3T	<i>Event-related</i>	Y	ROIs	6	N	Brain Voyager QX 2.3	Talairach
Guo et al. (2012)	12	19-31	Functional localizer	Pro-saccades > Fixation	3T	Blocked	Y	ROIs	6	N	SPM8	Talairach
Guo et al. (2018)	16	23.2	Functional localizer	Pro-saccades > Fixation	3T	Blocked	Y	FEF foci	2	N	Brain Voyager QX	Talairach
Heinen et al. (2006)	5	20-37	Functional localizer	Pro-saccades > Fixation	3T	Blocked	Y	ROIs	4	N	VISTASOFT	Talairach
Hohl et al. (2008)	7	31 ± 9	Functional localizer	Pro-saccades > Fixation	3T	Blocked	N	Whole-brain	9	N	Brain Voyager QX	Talairach
Jamadar et al. (2015)	23	25.8; 18-43	Functional localizer	Pro-saccades > Fixation	3T	<i>Event-related</i>	Y	Whole-brain	47	N	SPM8	MNI
Jamadar et al. (2015)	23	25.8; 18-43	Functional localizer	Anti-saccades > Fixation	3T	<i>Event-related</i>	Y	Whole-brain	47	N	SPM8	MNI
Jarvstad & Gilchrist (2019)	23	NA	Functional localizer	Pro-saccades > Fixation	3T	Blocked	Y	Whole-brain	4	N	FSL v.5.06-1	MNI
Kassner et al. (2007)	4	20-36	Functional localizer	Pro-saccades > Fixation	3T	Blocked	Y	ROIs	5	N	AFNI	Talairach
Kuzina et al. (2005)	6	29-38	Functional localizer	Pro-saccades > Fixation	3T	Blocked	N	Whole-brain	14	N	Advanced Visual Systems & AFNI	Talairach
Levy et al. (2007)	4	24-43	Functional localizer	Pro-saccades > Fixation	3T	Blocked	N	ROIs	5	N	Brain Voyager QX	Talairach
Neggers et al. (2007)	15	NA	Functional localizer	Pro-saccades & Anti-saccades > Fixation	3T	Blocked	N	ROIs	4	Y	SPM2	MNI
Pierce et al. (2019)	30	25.7 ± 4.1	Functional localizer	Pro-saccades > Fixation	3T	Blocked	Y	Whole-brain	9	Y	SPM12	MNI
Sehon et al. (2008)	17	21.29 ± 3.72	Functional localizer	Pro-saccades > Fixation	3T	Blocked	N	Whole-brain	19	N	SPM2	MNI
Schweidinger et al. (2013)	14	29.6 ± 9.6	Functional localizer	Pro-saccades & Anti-saccades > Fixation	3T	<i>Event-related</i>	Y	Whole-brain	10	Y	Brain Voyager QX 1.9	Talairach
Tanber-Rosenu et al. (2018)	8	28.5 ± 3.3	Functional localizer	Pro-saccades > Fixation	3T	Blocked	Y	ROIs	6	N	Brain Voyager QX v.1.10.2-2.8	Talairach
Tark & Curtis (2009)	5	22-39	Functional localizer	Pro-saccades > Fixation	3T	Blocked	Y	FEF foci	2	N	Caret	MNI
Tibber et al. (2010)	16	21-40	Functional localizer	Pro-saccades > Fixation	3T	Blocked	Y	ROIs	9	N	SPM5	Talairach
Tre et al. (2006)	10	27.9 ± 3.18	Functional localizer	Anti-saccades > Fixation	3T	Blocked	N	Whole-brain	21	N	SPM2	MNI

Table 2. List of the studies and contrasts included in the fPI localizer sample

Study	N	Age	Paradigm	Contrast	Scanner	Design	Eyetracker	Results reported for	N° of foci	fPI's activity lateralization	Software	Space
Ambrose et al. (2012)	20	23.5; 20-32	Task-switching paradigm	Task switch > Distractor trials	3T	<i>Event-related</i>	N	Whole-brain	15	Bilateral	SPM8	MNI
Ambrose et al. (2012)	20	23.5; 20-32	Task-switching paradigm	Distractor inhibition > Baseline	3T	<i>Event-related</i>	N	Whole-brain	9	Bilateral	SPM8	MNI
Ambrose et al. (2012)	20	23.5; 20-32	Task-switching paradigm	Task switch > Repetition trials	3T	<i>Event-related</i>	N	Whole-brain	13	Left	SPM8	MNI
Asplund et al. (2010)	30	NA	RSVP / Oddball paradigm	Surprise > Search trials	3T	<i>Event-related</i>	N	Whole-brain	17	Bilateral	Brain Voyager 4.0.1, OX 1.7.9	Talrach
Asplund et al. (2010)	30	NA	RSVP / Oddball paradigm	Search trials > Baseline	3T	<i>Event-related</i>	N	Whole-brain	8	Bilateral	Brain Voyager 4.0.1, OX 1.7.9	Talrach
Asplund et al. (2010)	6	NA	RSVP / Oddball paradigm	Search trials > Baseline	3T	<i>Event-related</i>	N	Whole-brain	8	Bilateral	Brain Voyager QX 1.11.4	Talrach
Asplund et al. (2010)	6	NA	RSVP / Oddball paradigm	Surprise > Search trials	3T	<i>Event-related</i>	N	ROIs	2	Bilateral	Brain Voyager QX 1.11.4	Talrach
Baldwin and Deshone (2014)	12	23-37	Object-based attention paradigm	Attend facehouse blocks > Difficultly-matched rare target detection	3T	Blocked	N	fPI only	7	NA	SPM8	MNI
Baldwin and Deshone (2014)	12	26.4; 24-30	Task-switching paradigm	Cue presentation > Baseline	3T	<i>Event-related</i>	N	Whole-brain	7	NA	SPM2	MNI
Baldwin and Deshone (2014)	12	26.4; 24-30	Task-switching paradigm	Target presentation > Baseline	3T	<i>Event-related</i>	N	Whole-brain	12	NA	SPM2	MNI
Baldwin and Deshone (2014)	12	26.4; 24-30	Task-switching paradigm	Response > Baseline	3T	<i>Event-related</i>	N	Whole-brain	9	NA	SPM2	MNI
Baltes et al. (2010)	18	23.4 ± 3.06; 18-28	Working memory paradigm	FC with fPI: Stimulus known > Stimulus unknown	3T	<i>Event-related</i>	N	Whole-brain	17	Right	SPM5	MNI
Baltes et al. (2010)	18	23.4 ± 3.06; 18-28	Working memory paradigm	FC with fPI: Stimulus known > Passive view + stimulus unknown	3T	<i>Event-related</i>	N	Whole-brain	17	Right	SPM5	MNI
Baltes et al. (2010)	11	26.2 ± 3.06	Task-switching paradigm	Cue-only trials > Null events	3T	<i>Event-related</i>	N	Whole-brain	22	Bilateral	LPISA	Talrach
Baltes et al. (2010)	11	26.2 ± 3.06	Task-switching paradigm	Cue-target > Cue-only trials	3T	<i>Event-related</i>	N	Whole-brain	21	Left	LPISA	Talrach
Baltes et al. (2010)	11	26.2 ± 3.06	Task-switching paradigm	Cue-target trials > Null events	3T	<i>Event-related</i>	N	Whole-brain	10	Bilateral	LPISA	Talrach
Baltes et al. (2010)	14	24.4 ± 1.9	Task-switching paradigm	Cue-target trials > No-cue-target trials	3T	<i>Event-related</i>	N	Whole-brain	9	Bilateral	LPISA	Talrach
Baltes et al. (2010)	14	24.4 ± 1.9	Task-switching paradigm	Meaning switch > Cue switch trials	3T	<i>Event-related</i>	N	ROIs	4	Left	LPISA	Talrach
Baltes et al. (2010)	14	24.4 ± 1.9	Task-switching paradigm	Cue switch > Cue repetition trials	3T	<i>Event-related</i>	N	ROIs	4	NA	LPISA	Talrach
Baltes et al. (2010)	14	24.4 ± 1.9	Task-switching paradigm	Switch > Repetition trials (single cue)	3T	<i>Event-related</i>	N	ROIs	3	Left	LPISA	Talrach
Baltes et al. (2010)	23	21 ± 1.67	Stroop paradigm	Stimulus incongruent > Baseline	3T	<i>Event-related</i>	N	Whole-brain	10	NA	SPM8	Talrach
Baltes et al. (2010)	23	21 ± 1.67	Stroop paradigm	Response incongruent > Stimulus incongruent (early stage)	3T	<i>Event-related</i>	N	Whole-brain	5	NA	SPM8	Talrach
Baltes et al. (2010)	23	21 ± 1.67	Stroop paradigm	Response incongruent > Stimulus incongruent (late stage)	3T	<i>Event-related</i>	N	Whole-brain	9	NA	SPM8	Talrach
Baltes et al. (2010)	9	19-42	Working memory paradigm	Target switching > Stimulus incongruent (late stage)	3T	<i>Event-related</i>	N	Whole-brain	12	Bilateral	Brain Voyager QX	Talrach
Baltes et al. (2010)	9	19-42	Working memory paradigm	Target switching > Non-switching trials (target non-occluded)	3T	Mixed blocked/event-related	N	Whole-brain	5	NA	Brain Voyager QX	Talrach
Casas et al. (2013)	18	28; 18-52	Object-based attention paradigm	High saliency maintained > attended stimuli	3T	<i>Event-related</i>	N	Whole-brain	5	Bilateral	SPM8	MNI
Casas et al. (2013)	19	20-36	Task-switching paradigm	Switch > Null event trials	3T	<i>Event-related</i>	N	fPI only	2	Bilateral	LPISA	Talrach
Casas et al. (2013)	19	20-36	Stroop paradigm	Incongruent > Neutral trials	3T	<i>Event-related</i>	N	fPI only	2	Bilateral	LPISA	Talrach
Casas et al. (2013)	19	20-36	Stroop paradigm	2-back > 0-back blocks	3T	Blocked	N	fPI only	2	Bilateral	LPISA	Talrach
Dehaene et al. (2002)	12	25.3 ± 2.4; 22-31	Stroop paradigm	Incongruent > Congruent trials	3T	<i>Event-related</i>	N	fPI only	1	Left	FSL	MNI
Dehaene et al. (2002)	14	20-32	RSVP paradigm	Discontinuous > Continuous & continuous-hard conditions	3T	<i>Event-related</i>	N	Whole-brain	14	Bilateral	Brain Voyager QX 1.10	Talrach
Dehaene et al. (2002)	14	20-32	RSVP / Oddball paradigm	Single-shot oddball trials > Search non-target trials	3T	<i>Event-related</i>	N	Whole-brain	7	Bilateral	Brain Voyager QX 2.3	Talrach
Dehaene et al. (2002)	14	20-32	RSVP / Oddball paradigm	Target > Distractor trials	3T	<i>Event-related</i>	N	Whole-brain	11	Bilateral	Brain Voyager QX 2.3	Talrach
Dehaene et al. (2002)	6	19-35	RSVP / Oddball paradigm	Target > Search trials	3T	<i>Event-related</i>	N	Whole-brain	11	Bilateral	Brain Voyager QX 2.3	Talrach
Dehaene et al. (2002)	6	19-35	RSVP / Oddball paradigm	Oddball > Search trials	3T	<i>Event-related</i>	N	Whole-brain	6	Bilateral	FSL	MNI
Dehaene et al. (2002)	25	25.5 ± 4.4	Working memory paradigm	2-back > 0-back trials (main effect)	3T	<i>Event-related</i>	N	Whole-brain	21	Bilateral	SPM8	MNI
Dehaene et al. (2002)	27	24.56 ± 2.53	Working memory paradigm	External attending to targets > Baseline	3T	Blocked	N	Whole-brain	7	NA	SPM2	MNI
Dehaene et al. (2002)	27	24.56 ± 2.53	Working memory paradigm	Internal orienting > Baseline	3T	Blocked	N	Whole-brain	8	NA	SPM2	MNI
Dehaene et al. (2002)	27	24.56 ± 2.53	Working memory paradigm	Internal > External attending (position task)	3T	Blocked	N	Whole-brain	15	Bilateral	SPM2	MNI
Dehaene et al. (2002)	16	23.6 ± 2.9; 18-35	Stroop paradigm	Task switch > Non-switch trials (main effect)	3T	<i>Event-related</i>	N	Whole-brain	20	Left	SPM5	MNI
Dehaene et al. (2002)	16	23.6 ± 2.9; 18-35	Stroop paradigm	Incongruent > Congruent trials (main effect)	3T	<i>Event-related</i>	N	Whole-brain	22	Bilateral	SPM5	MNI
Dehaene et al. (2002)	18	27.4 ± 6.6	Working memory paradigm	FC face cue and target > FC scene cue and target	3T	<i>Event-related</i>	Y	Whole-brain	9	Right	FSL	MNI
Dehaene et al. (2002)	18	27.4 ± 6.6	Working memory paradigm	Incongruent > Congruent trials	3T	<i>Event-related</i>	N	Whole-brain	13	NA	SPM2	MNI
Dehaene et al. (2002)	12	25.67 ± 1.88	Stroop paradigm	Word-oddball vs. Oddball control	3T	<i>Event-related</i>	N	Whole-brain	19	Bilateral	SPM2	MNI
Dehaene et al. (2002)	12	25.67 ± 1.88	Stroop paradigm	Color-oddball vs. Oddball control	3T	<i>Event-related</i>	N	Whole-brain	29	Bilateral	SPM2	MNI
Dehaene et al. (2002)	12	23; 19-34	Working memory paradigm	Sustained working memory > Sustained feature detection	3T	Blocked	N	Whole-brain	15	Left	AFNI	Talrach
Dehaene et al. (2002)	12	23; 19-34	Working memory paradigm	Update > Cue maintenance	3T	<i>Event-related</i>	N	Whole-brain	11	Left	AFNI	Talrach
Dehaene et al. (2002)	16	22; 18-32	Working memory paradigm	Memory > Rotation discrimination trials	3T	Blocked	N	Whole-brain	13	Right	AFNI	Talrach
Dehaene et al. (2002)	48	F: 22 ± 1.99; M: 22.6 ± 1.99	Task-switching paradigm	Task switch > Repetition trials	3T	<i>Event-related</i>	N	Whole-brain	5	Left	SPM5	MNI
Dehaene et al. (2002)	18	18-31	Working memory paradigm	Encoding period > Baseline	3T	<i>Event-related</i>	N	Whole-brain	27	Bilateral	Brain Voyager QX v1.09	Talrach
Dehaene et al. (2002)	22	18-30	Contingent capture paradigm	Silent target > Baseline	3T	<i>Event-related</i>	N	ROIs	13	Bilateral	AFNI	Talrach
Dehaene et al. (2002)	26	21.3; 21-25	Task-switching paradigm	Task switch > Repetition trials	3T	<i>Event-related</i>	N	Whole-brain	15	Left	SPM8	MNI
Dehaene et al. (2002)	13	25; 20-31	Working memory paradigm	FC with V4: Attend > Ignore color	3T	<i>Event-related</i>	N	Whole-brain	5	Right	SPM5	MNI
Dehaene et al. (2002)	13	25; 20-31	Working memory paradigm	FC with V5: Attend > Ignore motion	3T	<i>Event-related</i>	N	Whole-brain	8	Bilateral	SPM5	MNI
Zano et al. (2011)	20	24.25; 18-31	Working memory paradigm	FC with V4: Attend > Ignore color	3T	<i>Event-related</i>	N	Whole-brain	18	Right	SPM5	MNI
Zano et al. (2011)	20	24.25; 18-31	Working memory paradigm	FC with V5: Attend > Ignore motion	3T	<i>Event-related</i>	N	Whole-brain	16	Bilateral	SPM5	MNI
Zano et al. (2011)	19	19-26	Feature-based attention paradigm	Stimulus block > Baseline	3T	Blocked	Y	ROIs	8	Bilateral	Brain Voyager QX	Talrach
Zano et al. (2011)	13	21.54 ± 1.99	Working memory paradigm	High working memory load > Low working memory load	3T	<i>Event-related</i>	N	Whole-brain	7	Bilateral	SPM8	MNI

In summary, based on the evidence discussed above, in the IFJ sample, we included attentional (i.e., RSVP and endogenous cueing paradigms), working memory (primarily n-back paradigms), and cognitive control paradigms (i.e., task-switching and Stroop tasks; as it was done in Derrfuss et al. 2005). The main contrasts analyzed were therefore quite heterogeneous, but can be broadly grouped into the following primary ones (see Figure 2 for an overview of the selection procedure following the PRISMA2020 guidelines; Page et al. 2021; for the full list of studies and the related information see Table 2): 1. Oddball > Target trials in covert attention paradigms (e.g., RSVP paradigms); 2. Functional connectivity with a seed perceptual region (e.g., V4, V5, FFA) in the Attend > Ignore condition in n-back paradigms; 3. Switching > Repetition trials in task-switching paradigms; 4. Incongruent > Congruent trials in Stroop paradigms. With regards to the second contrast, we would like to note that even though these studies were based on second-level contrasts, as we were mainly interested in inferring the localization of the IFJ, we nevertheless decided to include them. This is because although these contrasts involve some form of masking (i.e., the restriction to a specific brain region for the assessment of the significance level, hence spatial bias), the anatomical regions that were used as seeds to run these analyses were posterior visual regions (e.g., V4, V5, and FFA), and their significant correlations were assessed over the whole-brain, making the localization of the IFJ with this method likely only slightly affected by this issue, if at all. Indeed, as previously suggested in Nee et al. (2013), their results match well those from traditional univariate analyses, and hence we decided to include them to increase statistical power (which was, as expected, lower than the FEF) and the representativeness of our main IFJ localizer sample. Given the heterogeneity of the contrasts included in the IFJ localizer sample, we also carried out an exploratory analysis by splitting up the sample according to the paradigm employed (i.e., oddball/cueing vs working memory paradigms vs task-switching and Stroop paradigms) to see whether these paradigms elicited activity in distinct regions near the putative IFJ and potential lateralization patterns. Task-switching and Stroop paradigms were grouped based on the results from Derrfuss et al. (2005).

In conclusion, the final sample of the included papers for our ALE meta-analysis was  $n = 51$  for the FEF, and  $n = 30$  for the IFJ sample (see Figures 1 and 2; Tables 1 and 2 for a summary of the studies; see Supplementary Tables 1, 2, and 3 for the control analyses). The number of experiments was 35 for the FEF sample, and 32 for the IFJ sample, which were both within the recommended sample size range (i.e., a minimum of 17-20 experiments) to have adequate statistical power with ALE as derived from empirical simulations (Eickhoff et al. 2016).

### **Activation likelihood estimation procedure**

After we extracted all the foci from the studies included in the FEF and IFJ sample, we converted all the Talairach coordinates to the MNI152 space using the Lancaster transform as implemented by the function provided in the GingerALE software (v. 3.0.2; Laird et al. 2010; Lancaster et al. 2007). We note that after the SPM2 version, the MNI templates distributed are consistent across FSL and SPM software packages, being compliant with the ICBM-152 coordinate space (Fonov et al. 2009), so for any later version of these packages we used the Talairach to MNI FSL transform. Where other software packages were used for spatial normalization, we again employed the Talairach to MNI FSL transform for consistency, as the other

transformation provided in GingerALE represents a pooled FSL/SPM transformation (Lancaster et al. 2007) that would only lead to systematic displacement of the coordinates. In only two cases (i.e., Manoach et al. 2007; Mao et al. 2007) the studies employed the mapping from MNI to Talairach developed by Brett et al. (2002). These coordinates were therefore mapped back to the MNI space using this specific transformation, as recommended in the GingerALE user manual.

For the main localizer analyses (FEF and IFJ localizer samples), the ALE parameters were set to 5000 threshold permutations and a voxel-level FWE of 0.01 was applied (Eickhoff et al. 2017) with a minimum cluster size of 50mm<sup>3</sup> (corresponding to 6 voxels). Compared to cluster-level FWE inference, which can only allow inferring that a given cluster is above a significance threshold as a whole, but critically, not that any putative region that is included in the cluster is individually significant on its own (Eickhoff et al. 2016), voxel-level FWE allows to more readily interpret all the cluster extent as well as its peak location from the main localizer samples anatomically (Eickhoff et al. 2016). Moreover, our sample sizes ensured that these clusters would not be driven by a contribution exceeding 50% of any individual study. Therefore we would like to stress that performing the ALE procedure for the main localizer samples using voxel-level FWE arguably represents the most conservative approach to inferring spatial convergence in our samples and allows us to interpret individual voxel ALE values as a proxy for the most active location across experiments. Since we were also interested in potential dissociations in the frontal cortex, this method therefore allows us to directly examine them. This is because in the case of samples lower than 10 studies (which corresponded to our the sample size for some of our control analyses), empirical simulation (Eickhoff et al. 2016) suggests that voxel-level FWE is more effective in reducing the contribution of any individual study to a given cluster location (with 8 studies, a single experiment can contribute to no more than 50% of the total ALE score), while with cluster-level FWE at least 17 to 20 studies would be necessary. As some of our studies also reported the results for ROIs only, our main inference will be aimed at interpreting the spatial relationship within FEF/IFJ rather than across the whole brain or the posterior PFC. However, in the case of regions that are under-reported in the literature (i.e., the iFEF), the use of a voxel-level FWE correction method may impose a too conservative threshold that would prevent us from detecting clusters of activity that are also consistently activated in the FEF sample (for instance, due to the fact that most studies where an FEF functional localizer was employed tend to report only a pair of bilateral foci, leaving out other regions potentially active in the task; see Table 1 for the studies that have only partially reported their results), thus biasing the results in favor of the main activation cluster. To compensate for this, in a control analysis, we therefore repeated the same ALE procedure on the FEF localizer sample setting the ALE parameters to an uncorrected p-value of 0.001, with 5000 threshold permutations and applying a cluster-level FWE of 0.01, which overall provides the best tradeoff between sensitivity and specificity to detect regions that may be under-reported (Eickhoff et al. 2017). For all the other control analyses (see FEF and IFJ sample inclusion criteria), the ALE parameters were set to 5000 threshold permutations and a voxel-level FWE of 0.01 with a minimum cluster size of 50mm<sup>3</sup> (corresponding to 6 voxels), as in our main localizer analyses. When retrieving the relevant foci, we first grouped the studies by subject group rather than by experiment (Turkeltaub et al. 2012). This was done because grouping by subject group further minimizes within-study effects (Turkeltaub et al. 2012). When a single experiment reported multiple contrasts of interest, we therefore pooled them under the same subject group. We note that however, in all cases in which the studies reported more than



one contrast of interest they were drawn from the same experiment (with very few exceptions; see Tables 1 and 2), so our strategy didn't unfairly pool together partially independent observations and was practically almost equivalent to grouping by experiment. When an experiment failed to report significant activation for some ROIs, we used the lower number of subjects that had above threshold activations in all ROIs from a contrast of interest if this information was available. In summary, our study grouping strategy allowed us to fully exploit the information gathered from the different contrasts that were performed in the original studies and also to carry out our control analyses with the largest possible sample sizes. To validate the results of the main ALE analyses and to further assess the reliability of the ALE peaks found, we also carried out a leave-one-experiment-out procedure (LOEO; Eickhoff et al. 2016) on the main FEF and IFJ localizer samples using the same foci grouping strategy. Since we found identical ALE peaks as in the main ALE analyses using 1000 threshold permutations, we performed the LOEO procedure with the same parameter to reduce computational times.

### **Comparison method of the ALE clusters with the MMP1, and relationship of the ALE peaks to gyral/sulcal information and previous coordinate-based meta-analyses**

To interpret our results more carefully, we compared the significant activation clusters from our ALE main localizer analyses with the results from previous meta-analyses results and brain atlases (Derrfuss et al. 2005; Glasser et al. 2016; Klein et al. 2012; Paus 1996). First, we described the macro-anatomical location of each cluster and assigned the corresponding Brodmann label with the Talairach Daemon that is implemented in GingerALE (Lancaster et al. 2000). Second, to compare our results with previous meta-analyses (Derrfuss et al. 2005; Paus 1996), we mapped our ALE peaks to the Talairach space using the transformation developed by Lancaster et al. (2007) as implemented in GingerALE (MNI (FSL) to Talairach; see Table 5). Third, in order to relate our results to surface-based atlases (Klein et al. 2012; Glasser et al. 2016), we followed two distinct approaches. The Mindboggle 101 atlas (Klein et al. 2012) describes the macro-anatomical organization of the human brain as delineated by sulcal and gyral information. The atlas was recently mapped to the MNI152 non-linear symmetric template (Manera et al. 2020), so we manually imported this atlas in FSL and in FSLeaves as described here ([The-Mindboggle-101-atlas-in-FSL](#)) and we assigned a Mindboggle 101 label to each of the ALE peak coordinates using the atlasquery command-line tool with FSL (v. 6.0.3). For atlases that were released and best interpreted in a surface-based framework (i.e., the MMP1 by Glasser et al. 2016; see Coalson et al. 2018 for an in-depth discussion), we instead employed the mapping technique developed in Wu et al. (2017) to register our ALE results from the MNI152 space (Fonov et al. 2009) to FSaverage (Fischl et al. 1999). A version of the MMP1 (Glasser et al. 2016) mapped to the FSaverage surface was made available using the method described in Mills (2016; [https://figshare.com/articles/dataset/HCP-MMP1\\_0\\_projected\\_on\\_fsaverage/3498446](https://figshare.com/articles/dataset/HCP-MMP1_0_projected_on_fsaverage/3498446)). Once we mapped the ALE clusters to this surface, we also mapped the MNI152 coordinates corresponding to each ALE peak to a vertex on the inflated surface (Wu et al. 2017) and we assigned each of these to the respective MMP1 labels (Table 5). When we needed to describe the anatomical labels associated with each ALE cluster using more specific labels (compared to the Talairach Daemon), we also used a volumetric version of this atlas for convenience. The source files that were used to import the atlas are the same as in Huang et al. (2021). This version was manually imported in FSLeaves as described here ([The-HCP-MMP1.0-atlas-in-FSL](#)).



## Meta-analytic connectivity modeling (MACM) method

After obtaining the ALE peaks from the main localizer analyses, we exploited this information to perform a data-driven analysis of the coactivation patterns of the FEF and the IFJ across the whole brain to uncover their task-based fMRI functional connectivity fingerprint (Langner and Camilleri 2021; Passingham and Wise 2002). We therefore retrieved all the papers matching specific criteria (described below) from the BrainMap database using Sleuth (<https://www.brainmap.org/sleuth/>; Fox and Lancaster 2002), and we analyzed these foci by employing the meta-analytic connectivity modeling (MACM) technique (Robinson et al. 2010). This technique leverages the ALE algorithm and allows inferring all the regions that coactivated with a given seed region that is selected a priori (and importantly, for which every included experiment has reported at least an activation peak within its boundaries). As a result, the seed regions will always show the highest activation convergence, but this analysis will also reveal all regions that coactivate above chance across the entire brain (Langner and Camilleri 2021). This analysis also allowed us to perform a reverse inference on these coactivation patterns (Poldrack 2011). More specifically, we sought to functionally decode and characterize the various behavioral domains that are associated above chance with each of these by using a standardized taxonomy (Fox et al. 2005) via the Mango software (v. 4.1) behavioral analysis plugin (v. 3.1; Lancaster et al. 2012). The studies were retrieved from the BrainMap database using Sleuth according to the following fields (all linked using the ‘AND’ operator) and specifications: in the Experiment field, the “context” field was set to “normal mapping”, in the “activation” field we searched for “activations only”, with “Imaging modality” being set to “fMRI”. Finally, four independent searches were conducted in the BrainMap database by setting the “locations” field as corresponding to each seed region (LH FEF, RH FEF, LH IFJ, and RH IFJ). We first transformed each seed location from MNI152 to Talairach space (which is the standard in Sleuth and also used internally by Mango’s behavioral plugin) using the transformation by Lancaster et al. (2007; the FSL transformation) and we created cuboid seeds of 6 mm centered around the respective ALE peaks. With these criteria, we were able to retrieve a range of 19 to 53 studies across seed locations. In particular, we retrieved 26 studies for the LH FEF seed, 19 studies for the RH FEF seed, 53 studies for the LH IFJ, and 31 studies for the RH IFJ. We note that the different number of studies retrieved possibly reflects a combination of the increased base probability of finding activations within a specific ROI (Langner et al. 2014; for example, foci within the LH IFJ seem to be reported more often throughout the BrainMap database, regardless of the specific fMRI paradigm) but also possibly the fact that some ROIs tend to participate in multiple functional networks (Langner and Camilleri 2021). Thus, while our sample size was generally greater in the case of the IFJ, this information matches what was previously reported about the coactivation patterns of FEF and IFJ (the IFJ being part of the frontoparietal network, that has been previously shown to work as a hub network; Cole et al. 2013), and more importantly, allowed for adequately powered inference using ALE (Eickhoff et al. 2016). Therefore, we used all the foci retrieved from each seed location, transformed in MNI152 space, as inputs for GingerALE. The ALE parameters were set to an 0.001 uncorrected p-value, 1000 threshold permutations and a cluster-level FWE of  $p < 0.01$ . In the functional decoding analysis, we used the same 6 mm cuboid seeds as in the MACM analysis centered around the

respective FEF and IFJ ALE peaks. Associations with behavioral domains were considered statistically significant when their z-score was  $\geq 3$ , corresponding to a threshold of  $p < 0.05$  (Bonferroni corrected).

## Data availability

The results of this study will be made available in NeuroVault (<https://neurovault.org/>) upon article acceptance.

# Results

## FEF and IFJ localizer samples ALE main clusters

In the FEF localizer sample, the activations converged most strongly in two main clusters localized in the left and right posterior dorsolateral PFC. Two ALE peaks were found near the junction of the sPCS with the SFS, localized in the anterior (in the left hemisphere) and posterior (in the right hemisphere) banks of the sPCS (Figure 3). These peaks match well the classical description of the human FEF as inferred with fMRI (Petit and Pouget 2019; Vernet et al. 2014). Our LOEO procedure overall confirms the reliability of the localization of these ALE peaks (see Table 5; LH: 26/35; RH: 23/35). In the IFJ localizer sample, the activations converged more strongly in two main clusters localized in the left and right posterior ventrolateral PFC. These clusters extended both in the dorsal and ventral portion of the iPCS, partially encroaching on the IFS (see Figure 3). The cluster in the right hemisphere was slightly more focused spatially compared to the cluster in the left hemisphere. Crucially, in both clusters, we found that the ALE peaks were localized along the posterior bank of the iPCS, near its ventral junction with the IFS, which closely matches the description of the IFJ (Derrfuss et al. 2005; Muhle-Karbe et al. 2016). Again, our LOEO procedure overall suggests that these ALE peaks are highly reliable across experiments (see Table 5; LH: 31/32; RH: 24/32).

## FEF sample ALE results - FEF lateral peak and other significant clusters

In the left hemisphere, we also found a lateral peak within the FEF cluster, which was localized on the bank of the iPCS, dorsal to its junction with the IFS. This lateral peak corresponds to what has been previously referred to as the inferior or the lateral FEF (see Figure 4; Derrfuss et al. 2012; Kastner et al. 2007; Luna et al. 1998). In addition to the main FEF clusters in the left/right PFC, the ALE technique revealed three other clusters that were consistently activated when subjects performed prosaccades and antisaccades contrasted against a fixation baseline across experiments. These clusters were localized in the medial frontal gyrus and the left/right posterior parietal cortex (Table 3). The cluster in the medial frontal gyrus comprised both the supplementary and the cingulate eye field (SCEF; Amiez and Petrides 2009) and the dorsal cingulate motor cortex (Glasser et al. 2016). In the posterior parietal cortex, two bilateral superior clusters spanned the precuneus and the SPL (Scheperjans et al. 2008a, 2008b), and an additional cluster was found in the right anterior intraparietal area (Glasser et al. 2016; Numssen et al. 2021).

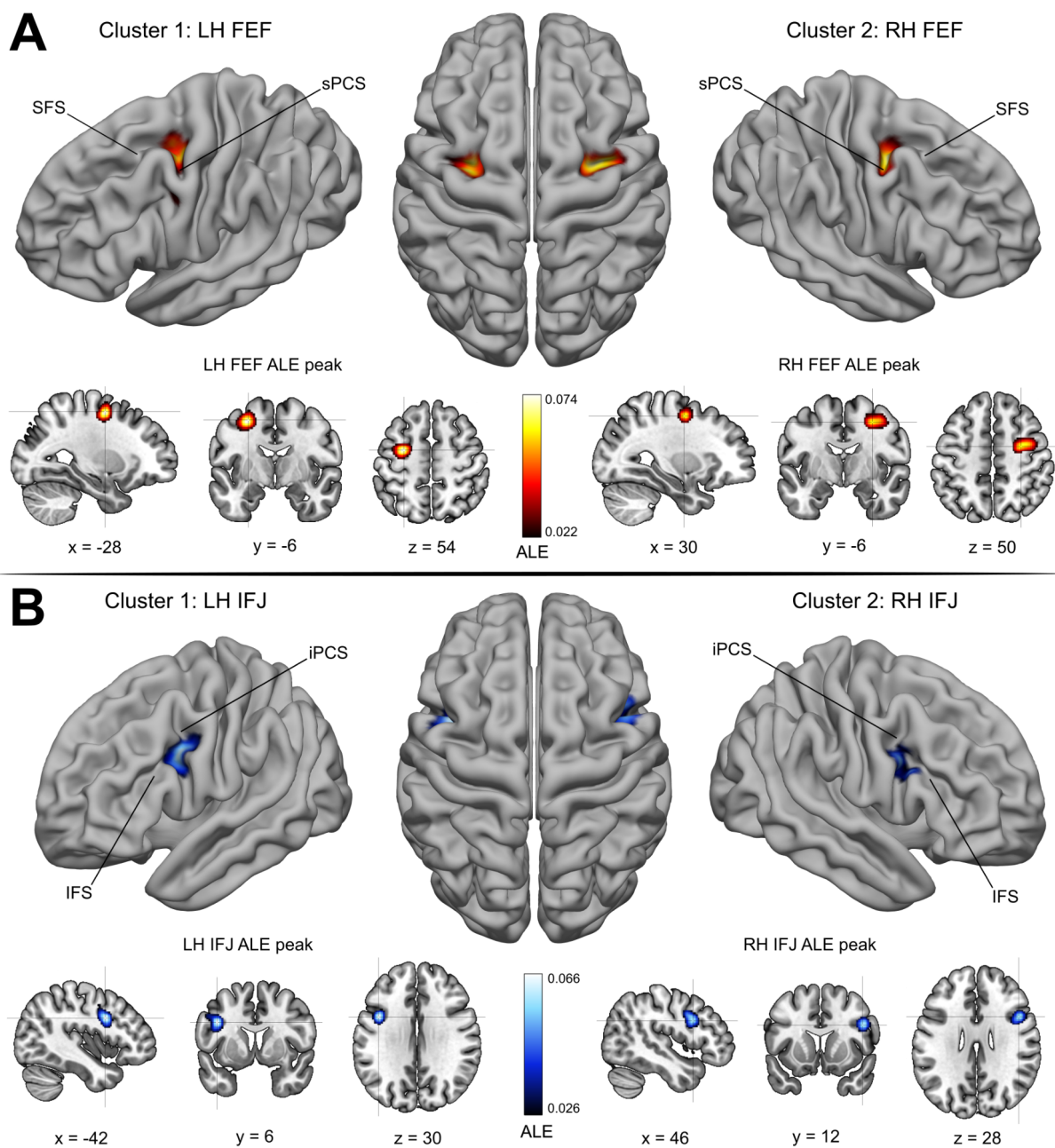


**Figure 3.** FEF and IFJ localizer samples - ALE main clusters. Panel A shows the ALE results from the FEF localizer sample. Two main clusters were found in the posterior dorsolateral PFC, closely matching the description of the anatomical location of the FEF (Paus 1996; Vernet et al. 2014). The FEF peaks were localized at the junction of the sPCS with the SFS, in the anterior (in the left hemisphere) and posterior (in the right hemisphere) banks of the former. Panel B shows the ALE results from the IFJ localizer sample. Again, two main clusters were found in the posterior ventrolateral PFC, and their respective peaks were localized along the posterior bank of the iPCS, near its ventral junction with the IFS. The location of these peaks and the corresponding MNI coordinates match the description of the IFJ (see also Table 4 and 5; Derrfuss et al. 2005; Muhle-Karbe et al. 2016).

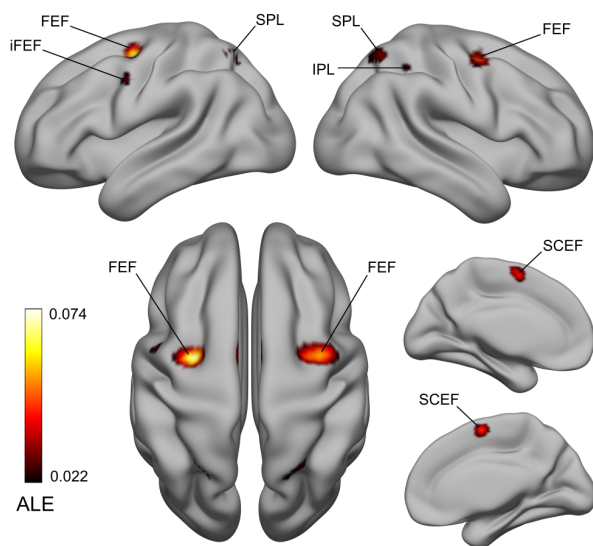


**Figure 4.** FEF sample ALE results - FEF lateral peak and other significant clusters. In the FEF localizer analysis, we also found a lateral peak in the left hemisphere, which was localized near the bank of the iPCS, dorsal to its junction with the IFS, corresponding to the inferior or lateral FEF. It is debatable however whether this region should be considered part of the FEF proper (Glasser et al. 2016; Mackey et al. 2017). Other significant clusters were localized in the supplementary and cingulate eye field (SCEF) and the dorsal cingulate motor cortex, and in the precuneus/SPL and the right anterior intraparietal area.

**Table 3.** FEF localizer sample ALE results

Cluster	Macroanatomical location	Hemi	MNI152 coordinates			ALE value	Volume (mm <sup>3</sup> )	BA
			x	y	z			
1	Precentral Gyrus	L	-28	-6	54	0.0736	4960	6
	Precentral Gyrus	L	-48	-2	40	0.0293		6
2	Precentral Gyrus	R	30	-6	50	0.0624	4304	6
3	Medial Frontal Gyrus	L/R	0	0	58	0.0548	3088	6
4	Precuneus	L	-22	-58	56	0.0418	1568	7
5	Precuneus	R	24	-60	56	0.0376	1104	7
6	Inferior Parietal Lobule	R	36	-46	48	0.0262	176	40

Importantly, by repeating the ALE analysis using cluster-level FWE (control analysis 1: see Materials and methods), we were able to uncover bilateral activations ventral to the main FEF peaks (see Supplementary Figure 1). These activations were extending from the sPCS to the posterior bank of the iPCS and were primarily localized in the iPCS (see Supplementary Figure 1), thus revealing the presence of bilateral iFEF peaks. Finally, our two additional control analyses show evidence of important spatial segregation and overlap near the putative FEF for antisaccades, prosaccades and covert spatial attention contrasts (see Supplementary Figures 2 and 3). As previously reported by other studies (Cieslik et al. 2016; Jamadar et al. 2013), the antisaccade > prosaccade contrast seemed to activate partially segregated clusters relative to prosaccade > fixation contrasts. While in the right hemisphere, the antisaccade cluster was more medial and anterior to the prosaccade cluster, overlapping at the junction of the sPCS with the SFS, this organization was less evident in the left hemisphere, where the two clusters overlapped near the same anatomical location, with a segregated cluster for antisaccades localized rostrally. Additionally, in this hemisphere, the ALE peaks for pure prosaccades > fixation contrasts and the main localizer sample coincided ( $x=-28$ ,  $y=-6$ ;  $z=54$ ; MNI152 coordinates). However, in the right hemisphere there were two ALE peaks for prosaccades ( $x=36$ ,  $y=-4$ ;  $z=52$ , and  $x=30$ ,  $y=-4$ ;  $z=50$ , the second of which was only slightly anterior to the ALE peak from the main localizer sample;  $x=30$ ,  $y=-6$ ;  $z=50$ , all MNI152 coordinates), overall showing greater uncertainty along the lateral axis in this hemisphere. The comparison of prosaccades and covert spatial attention activations (see Supplementary Figure 3) reveals a clear pattern of overlap near the

junction of the sPCS and SFS, consistent with the hypothesis that covert and overt attention have a spatially common source within the FEF (Astafiev et al. 2003; Corbetta et al. 1998; de Haan et al. 2008), with the disjunctions in covert attention being mostly localized in the posterior bank of the sPCS in both hemispheres.

## IFJ sample ALE results - Other significant clusters

By carrying out a pooled analysis of fMRI experiments using feature- and object-based attention (with manipulations of both top-down and bottom-up factors), working memory, and cognitive control (i.e., task-switching and Stroop) paradigms, the ALE technique revealed consistent activations in eight clusters forming a broad fronto-parietal network (see Figure 5). In addition to the main IFJ clusters in the left/right PFC, we found several other consistently activated clusters in the frontal cortex: the first was localized in the medial frontal in the bilateral SCEF (Amiez and Petrides 2009), a second in the left precentral gyrus (within the putative FEF), and finally, two other clusters were localized in the bilateral insular cortex and claustrum (Table 4). Posteriorly, we also found a cluster in the left SPL/IPL, and a smaller cluster in the right SPL/IPL (Numssen et al. 2021; Scheperjans et al. 2008a, 2008b). These clusters do not support only a single cognitive function and there isn't a clear overlap with recent rs-fMRI network topography, although all the clusters belong to the cognitive control network (Cole et al. 2007). These networks of areas may be tentatively described as associated with the "encoding and updating of task-relevant representations" as proposed in Derrfuss et al. (2005). Critically, by splitting up our sample based on the paradigm employed (i.e., oddball/cueing vs n-back vs task-switching/Stroop), we found interesting dissociations within the putative IFJ as well as lateralization patterns (see Supplementary Figure 4). Starting with the latter, while oddball/cueing paradigms gave rise to bilateral activations near the putative IFJ, working memory paradigms activated a cluster in the right hemisphere, whereas the opposite was true for task-switching/Stroop paradigms, which resulted in a cluster of activity in the left hemisphere only. Remarkably, each of these clusters had a quite distinct spatial topography. In the left hemisphere, the cluster related to cognitive control (task-switching + Stroop paradigms) was extending from the posterior bank of the superior iPCS to the junction of the iPCS with the IFS, where it overlapped with the oddball/cueing cluster. This cluster further extended anteriorly and ventrally at this same anatomical location. The same arrangement was approximately found in the right hemisphere, in which a posterior-dorsal working memory limited cluster overlapped with the oddball/cueing cluster just above the junction of the iPCS with the IFS. The oddball/cueing cluster again extended anteriorly and ventrally.

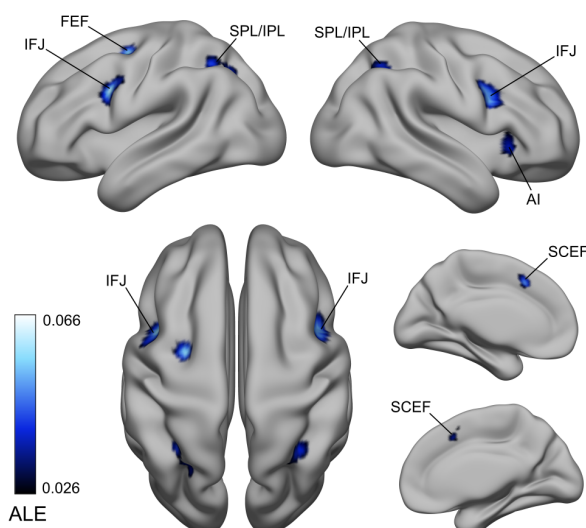


**Figure 5.** IFJ sample ALE results - Other significant clusters. In addition to the bilateral IFJ clusters, we found significant activations in the SCEF, the left FEF, in two clusters in the insular cortex and claustrum (not visible in the left hemisphere), and finally, in the SPL/IPL. Given that these areas were responding across many different paradigms, we suggest that they could be associated with the "encoding and updating of task-relevant representations" as first proposed in Derrfuss et al. (2005), and belong to the cognitive control network (Cole et al. 2007).



**Table 4.** IFJ localizer sample ALE results

Cluster	Macroanatomical location	Hemi	MNI152 coordinates			ALE value	Volume (mm <sup>3</sup> )	BA
			x	y	z			
1	Precentral Gyrus	L	-42	6	30	0.0658	3488	6
2	Inferior Frontal Gyrus	R	46	12	28	0.0597	3016	9
3	Medial Frontal Gyrus	L	-2	18	44	0.0574	2328	6
4	Superior Parietal Lobule	L	-30	-54	48	0.0445	1504	7
	Precuneus	L	-26	-66	44	0.0388		7
5	Precentral Gyrus	L	-28	-4	54	0.0578	1208	6
6	Superior Parietal Lobule	R	34	-56	48	0.0408	800	7
7	Clastrum	R	32	22	-2	0.0386	728	*
8	Clastrum	L	-30	18	2	0.0343	424	*

## Spatial relationship of the significant clusters with previous coordinate-based meta-analyses, macro-anatomical information and the MMP1

The comparison of the FEF and IFJ ALE peaks from the localizer samples analyses overall shows good spatial correspondence with results from previous meta-analyses and the MMP1 (Glasser et al. 2016), but with some important differences that are worth examining in detail (see Table 5). The FEF ALE peaks from our results are localized much more medially and posteriorly relative to the results reported in Paus (1996), highlighting marked spatial differences with this landmark FEF meta-analysis (which however was based on PET evidence). In contrast, the IFJ ALE peaks are virtually identical to those reported in the study by Derrfuss et al. (2005; but with slightly less agreement in the right hemisphere), where the authors also employed the ALE technique in one of its earlier implementations. Macro-anatomically, according to the Mindboggle 101 atlas (Klein et al. 2012; Manera et al. 2020), the LH FEF and RH FEF peaks lie within the caudal middle frontal gyrus (in BA 6; see Table 3) and not in the precentral gyrus, as previously assumed based on non-human primate evidence (Bruce et al 1985; Schall et al. 2020, and Tehovnik et al. 2000, for reviews). These results are consistent with the few pieces of evidence available on the delineation of this region based on cytoarchitecture in *post-mortem* studies (Rosano et al. 2003; Schmitt et al. 2005). While the left IFJ ALE peak was found in the precentral gyrus (in BA 6; see Table 5), which also agrees well with cytoarchitectonic criteria (Amunts and Von Cramon 2006), interestingly the right IFJ ALE peak was instead localized within the pars opercularis (in BA 9).

**Table 5.** Comparison of the ALE peaks with previous meta-analyses and brain atlases

Cluster	Hemi	ALE peaks			Talairach coordinates			Previous meta-analyses (Talairach space)						Brain atlases Mindboggle 101 Label	MMP1 Label	LOEO results ALE peak ratio
		MNI152 coordinates			x	y	z	Paus (1996)			Derrfuss et al. (2005)					
		x	y	z				x	y	z	x	y	z			
FEF	L	-28	-6	54	-27.73	-9.61	51.32	-32	-2	46	//	//	//	Caudal Middle Frontal Gyrus	i6-8	26/35
FEF	R	30	-6	50	27.17	-9.86	48.03	31	-2	47	//	//	//	Caudal Middle Frontal Gyrus	6a	23/35
IFJ	L	-42	6	30	-40.87	3.27	30.37	//	//	//	-40	4	30/32	Precentral Gyrus	6r	31/32
IFJ	R	46	12	28	42.43	8.35	29.4	//	//	//	44	10	34	Pars Opercularis	6r	24/32

Finally, in our opinion the most interesting results of these comparisons were those obtained from the projection of our main FEF and IFJ clusters on the FSaverage surface using the method from Wu et al. (2017; see Materials



and methods) where we could precisely assess their spatial relationship with the MMP1 (Glasser et al. 2016; see Figure 6). The FEF clusters covered almost the entire middle and anterior part of the FEF (as defined by the corresponding MMP1 label) but also large parts of the middle and posterior 6a region. Moreover, the left and right hemisphere ALE peaks were found within area i6-8 and area 6a, anteriorly and dorsally relative to the FEF, respectively. The IFJ clusters instead spanned multiple MMP1 labels, including areas PEF, 6r, IFJp and IFJa. While in the left hemisphere, the majority of the vertices of the cluster seemed to be localized in the middle and posterior aspect of the IFJp, in the right hemisphere most of the vertices were localized in the ventral 6r region. Crucially, in both hemispheres however, the ALE peaks were localized in this region (i.e., 6r), ventrally relative to the IFJp. We offer an interpretation of potential reasons for these discrepancies in the discussion section.

### **Meta-analytic connectivity modeling (MACM) results**

The MACM analysis of the FEF and IFJ revealed a broad set of regions that coactivated with these seeds in the BrainMap database (see Figure 7) encompassing the frontal, parietal and temporal cortices. The LH FEF seed coactivated with other six clusters (see Figure 7, panel A), and the RH FEF coactivated with other eight clusters (Figure 7, panel B). Interestingly, while these FEF coactivations included as expected medial oculomotor regions (the SCEF) and the SPL/IPL, in both analyses we found coactivated clusters in the bilateral ventral PFC, which included parts of the iFEF and the IFJ based on their localization with respect to the iPCS and the IFS. Instead, the LH IFJ coactivated with a broad set of other nine clusters (Figure 7, panel C), and the RH IFJ coactivated with only five other clusters (Figure 7, panel D). The coactivations of these bilateral seeds spread onto the IFS and ventrally in the insular cortex and claustrum. Again, these coactivations included clusters in the SCEF, and the SPL/IPL and angular gyrus. In contrast to the FEF coactivations, where the bilateral IFJ was always coactivated, we did not find FEF coactivations in the IFJ MACM results, with the exception of the ipsilateral FEF in the LH IFJ MACM analysis. Another crucial difference was that in this analysis, we found a large cluster in the left temporal lobe that included the fusiform gyrus and the inferior occipital cortex. To summarize, while the FEF MACM analysis shows that this region is consistently coactivated with the ventrolateral PFC and regions in the posterior parietal cortex across paradigms, the IFJ has more widespread whole-brain coactivation patterns (particularly in the left hemisphere), being more strongly connected with the rest of the PFC and with the insular cortex and claustrum, and possessing a differential connectivity pattern with the inferior temporal cortex, which was completely lacking in the case of FEF. In addition to revealing the task-based functional connectivity fingerprints of these regions (i.e., the coactivation patterns, as reported above), our functional decoding approach in BrainMap allowed us to uncover the behavioral domains significantly associated with each of them. Performing such reverse inference on the coactivation patterns of the LH FEF showed that the prevalent association was in the ‘action’ behavioral domain (see Figure 7, right side of panel A), namely execution.unspecified. In the ‘cognition’ domain, there were four prominent associations with attention, working memory, reasoning and spatial cognition. Finally, in the ‘perception’ domain, the two highest associations were with vision.motion and vision.shape.

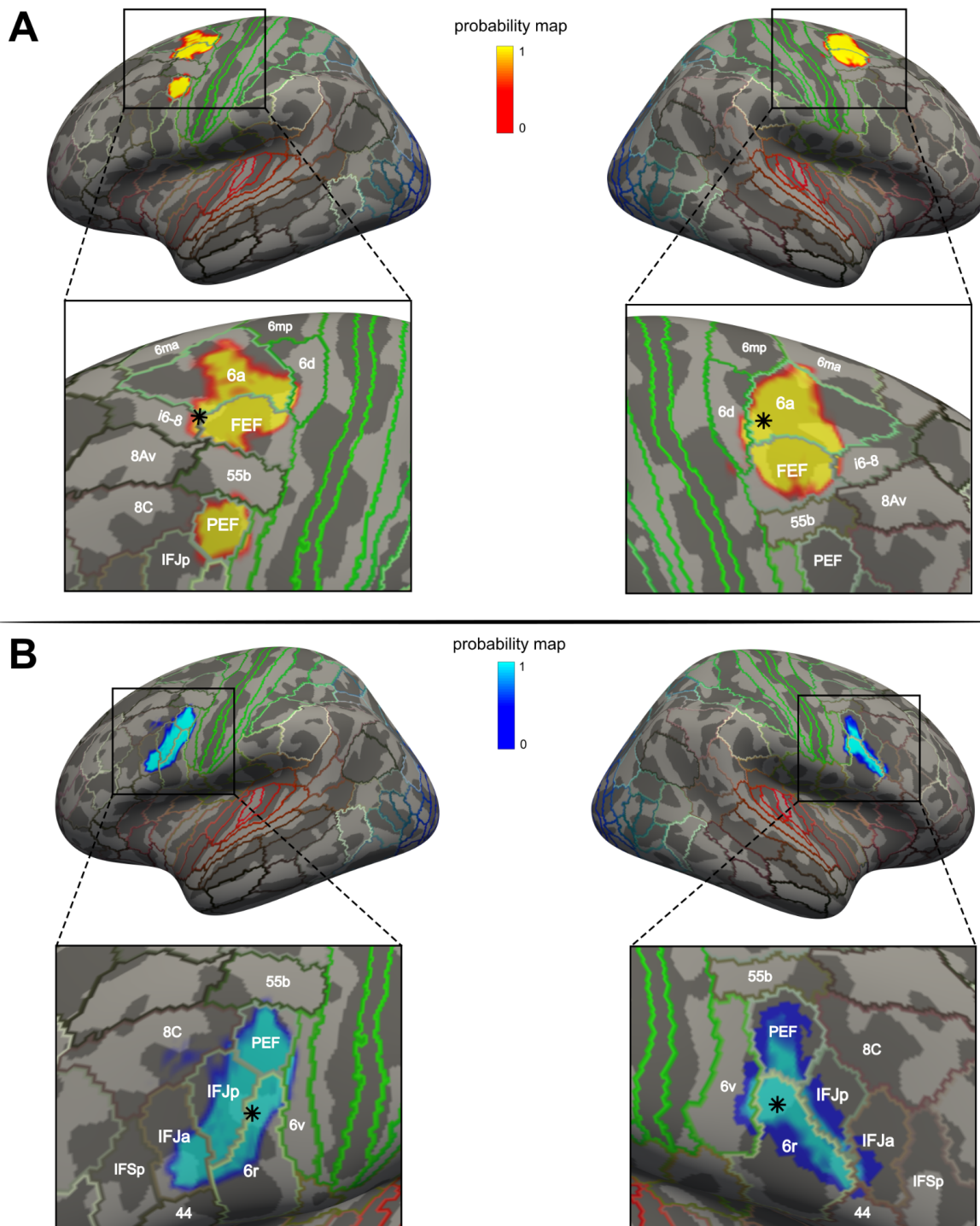


**Figure 6.** Projection on FSaverage of the FEF and IFJ main clusters and comparison with the MMP1 taxonomy. Panel A shows the vertices corresponding to the FEF clusters. Both clusters cover the middle and rostral part of the FEF label as defined according to the MMP1 atlas, but they also cover large parts of area 6a. In the left, hemisphere, vertices were also localized in the iFEF, which matches almost exactly the boundaries of area PEF from the atlas. The LH FEF peak was localized within area i6-8, just anterior to the FEF, and the RH FEF peak was localized within area 6a, dorsal to FEF. Despite this difference, both peaks were localized near the junction of the sPCS and the SFS, in the anterior bank and the posterior banks of the sPCS, respectively. Panel B shows the vertices corresponding to the IFJ clusters. They showed a similar elongated shape that approximately followed the posterior iPCS and encroached onto the IFS, and they spanned multiple MMP1 areas. Importantly, we found that in both hemispheres the IFJ peaks were localized near the junction of the iPCS and the SFS within area 6r, posteriorly to the IFJp.

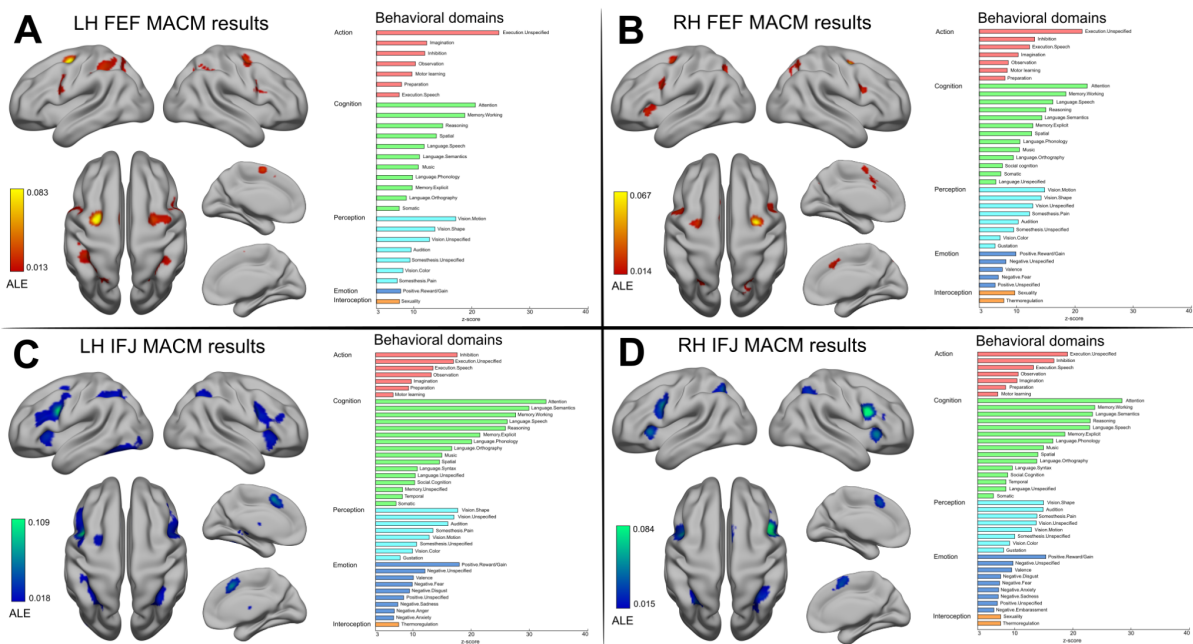


**Figure 7.** Meta-analytic connectivity modeling results (MACM) and histograms of the significant associations with behavioral domains ( $p < 0.05$ , Bonferroni corrected). Panel A and B depict the coactivation profiles of the FEF, and Panel C and D the coactivation profiles of the IFJ.

The behavioral domain associations with the coactivation patterns of the RH FEF (see Figure 7, right side of panel B) were very similar to the LH FEF. Again, the primary association in the ‘action’ domain was with execution.unspecified. The prevalent association was however in the ‘cognition’ domain with attention, followed by working memory, language.speech and by reasoning. As for the previous seed, the two highest associations were with vision.motion and vision.shape in the ‘perception’ domain. The functional decoding of the LH and RH IFJ coactivation patterns uncovered associations with similar behavioral domains, although with some interesting differences in their predominance. The LH IFJ coactivations had the highest association with attention in the ‘cognition’ domain (see Figure 7, right side of panel C), followed by language.semantics, working memory, and language.speech. The next strongest association was in the ‘emotion’ domain with positive.reward/gain. Then, there were significant associations in the ‘perception’ domain with vision.shape and vision.unspecified and audition. Finally, in the ‘action’ domain we found the most prevalent associations with inhibition and execution.unspecified. As for the previous seed, the RH IFJ had the highest association with attention in the ‘cognition’ domain (see Figure 7, right side of panel D). In the same domain, there were also strong associations with working memory, language.semantics, reasoning, and language.speech. Next, we found two prominent associations in the ‘action’ domain with inhibition and execution.unspecified. Again, we found an association with positive.reward/gain in the ‘emotion’ domain. Lastly, the strongest associations in the ‘perception’ domain were with vision.shape, audition and somesthesia.pain.

## Discussion

The PFC is essential to several aspects of flexible goal-driven behavior that are mediated by specialized brain regions (Fuster 2000; Miller and Cohen 2001). The FEF and the IFJ have been previously implicated in covert and overt spatial attention on the one hand (Corbetta et al. 1998; Vernet et al. 2014), and working memory and cognitive control on the other (Bedini and Baldauf 2021; Brass et al. 2005), and their localization has been traditionally associated with the major sulci of the posterior-lateral PFC, namely the SFS and the sPCS, and the iPCS and the IFS, respectively (Brass et al. 2005; Paus 1996). Due to the large body of empirical work that has accumulated over the past years on these regions (Bedini and Baldauf 2021) and the parallel development of more robust meta-analytic techniques for neuroimaging data (Fox et al. 2014), we felt the need to reassess previous results in light of the current evidence, with a specific focus on overcoming discrepancies in the definition and localization of these regions using fMRI in humans. In particular, in this study, we sought to accurately estimate the precise localization of these regions in standard space by performing a coordinate-based meta-analysis using the ALE technique (Eickhoff et al. 2012). To model the spatial convergence of activations within the FEF, we analyzed data from 35 fMRI studies (35 experiments) that investigated the planning and execution of prosaccades and antisaccades contrasted against a fixation baseline in over 400 subjects. To model the spatial convergence within the IFJ, we analyzed data from 30 fMRI studies (32 experiments) that investigated visual attention, working memory, and cognitive control, in over 500 subjects. Overall, our results revealed a network of regions including the FEF, which is involved in top-down and bottom-up spatial attention and oculomotor control, as shown by previous studies (Grosbras et al. 2005; Jamadar et al. 2013; Luna et al. 1998), as well as a network of regions including the IFJ that may be generally characterized as being involved in encoding and updating task-relevant representations (Cole and Schneider 2007; Derrfuss et al. 2005). Crucially, we found that by modeling activity across studies (thus partially overcoming inter-individual variability), sulcal landmarks are indeed consistently associated with both regions, as indicated by the location of the ALE peak values. Our results thus suggest a robust association of structure and function in these higher regions (Frost and Goebel 2012; Miller et al. 2021; Van Essen 2007; Wang et al. 2015), similarly to what previous studies have shown in early to mid-level visual regions (Benson et al. 2012; Hinds et al. 2008, 2009), which we suggest should be examined by future fMRI studies more systematically at the individual-subject level (Amiez and Petrides 2018; Derrfuss et al. 2009, 2012).

The FEF is arguably one of the most important regions of a network involved in the planning and execution of saccadic eye movements that have been extensively studied in primates (Schall and Thompson 1999; Tehovnik et al. 2000). In humans, this network usually comprises a set of regions in the lateral and medial frontal cortex, posterior parietal cortex, and subcortical nuclei (Corbetta et al. 1998; Grosbras et al. 2005), and has been mainly investigated with fMRI over the past 25 years, enabling to characterize their respective functions (McDowell et al. 2008). Following the crucial foundation set by primate neurophysiology (Bruce et al. 1985; Buschman and Miller 2009; Moore and Fallah 2001), the human FEF has often been seen as not only implicated in the production of visually-guided and voluntary saccades and other oculomotor behaviors (Schall 2015), but also in covert shifts of spatial attention, spatial working memory, and more complex executive functions (Corbetta et al.



1998; Fiebelkorn and Kastner 2020; Vernet et al. 2014). The localization of the human FEF is however highly debated and affected by strong spatial variability (see Bedini and Baldauf 2021 for a discussion), possibly due to inter-individual differences that are obscured when only reporting group-level results. In most of the previous fMRI research, the gold standard FEF functional localizer consisted of tasks alternating blocks of visually-guided saccades with fixation blocks (Amiez et al. 2006; Amiez and Petrides 2018). This blocked design approach is often seen as complementary to another approach that uses the anti-saccade task (Connolly et al. 2000; Munoz and Everling 2004). This task elicits activity in a broader set of regions in the dorsolateral PFC when contrasted with a fixation baseline (Connolly et al. 2000; McDowell et al. 2008), and it may therefore potentially be less specific to localizing the FEF. Some studies suggest however that these additional areas are recruited during the preparatory period, rather than the response period (see Curtis and D'Esposito 2003; Ford et al. 2005), and that the increased activity that is observed throughout the oculomotor network may be further exacerbated by mixed vs blocked behavioral designs (i.e., prosaccades mixed with antisaccades trials; Pierce and McDowell 2016, 2017) and modulated by inter-trial effects in the FEF (Manoach et al. 2007). Furthermore, several studies reported activation within the FEF (defined in a separate localizer scan) in the antisaccade and prosaccade tasks (Brown et al. 2006, where again activity is particularly elevated throughout the preparatory period; De Souza et al. 2003; Furlan et al. 2016). Previous coordinate-based meta-analyses that used the ALE technique have also provided evidence of the consistency of the clusters of activity found across individual fMRI and PET experiments investigating prosaccades and antisaccades (Cieslik et al. 2016; Grosbras et al. 2005; Jamadar et al. 2013). However, given the inherent spatial coarseness of the localization derived from PET and low-resolution MRI scanners (i.e., 1.5T) and acquisition methods that were included in these previous meta-analyses, these studies were only partially able to accurately infer spatial convergence across experiments, as well as dissociations across paradigms and contrast. In addition, since some of these studies relied on earlier implementations of the ALE technique, which allowed for within-study effects (see Turkeltaub et al. 2012), and critically, more liberal statistical thresholds and multiple comparisons correction solutions (such as false discovery rate, which is no longer recommended, as it is not considered appropriate for spatial inference; Eickhoff et al. 2016), these studies may have potentially overestimated the statistical evidence of spatial convergence and segregation between clusters of activity in their samples. Finally, another aspect that is difficult to evaluate retrospectively was the reporting of an implementation error in an earlier ALE version (Eickhoff et al. 2017), which practically led to bypassing the multiple comparisons correction step, and which may therefore have affected the meta-analyses previous to that report (Eickhoff et al. 2017). In this study, we attempted to overcome some of these limitations by applying a conservative thresholding method and by including higher resolution fMRI studies (i.e., 3T or 4T) to accurately infer the localization of the human FEF in standard space. Our ALE results, obtained by analyzing prosaccades > fixation, antisaccades > fixation, and prosaccades and antisaccades > fixation contrasts across 35 fMRI experiments (see Table 3), show that the highest spatial convergence based on the ALE value was found within two bilateral clusters in the dorsolateral PFC, localized in the anterior bank of the sPCS, near its junction with the SFS (see Figure 3; Table 2). Both clusters of activity were localized in Brodmann Area 6, and the respective peak localization is consistent with the few *ex-vivo* data available (see in particular Rosano et al. 2003, Figure 7; and Schmitt et al. 2005), consolidating the notion that the FEF is typically localized in a transition area between the granular and agranular tissue within PFC (sometimes referred to as dysgranular cortex; Petrides and Pandya 1999). The ALE peak coordinates are much

more posterior and slightly more lateral than those reported in Paus (1996; see Table 5). Macro-anatomically, they are both localized within the caudal middle frontal gyrus (Klein et al. 2012; Manera et al. 2020), although the clusters extend also posteriorly in the precentral gyrus and dorsally in the superior frontal gyrus (see Blanke et al. 2000, for similar results based on electrical stimulation). Our comparison with one of the most comprehensive brain parcellations available to date, namely the MMP1 (Glasser et al. 2016), revealed some interesting spatial patterns. While many of the projected voxels of our FEF clusters were localized within the middle and anterior part of the MMP1 FEF region, a considerable portion was also spreading dorsally in the middle and posterior 6a region. Furthermore, the ALE peaks were localized within area i6-8 in the left hemisphere, and area 6a in the right hemisphere according to the MMP1. In the left hemisphere, a ventral cluster corresponding to the inferior or lateral FEF (Derrfuss et al. 2012; Kastner et al. 2007; Luna et al. 1998) overlapped almost entirely with the PEF. These results suggest that there may be important differences in the way the FEF is defined across methods. The MMP1 was created by a careful manual delineation combining structural MRI (cortical thickness and myelin ratio), resting-state fMRI connectivity and retinotopic mapping techniques (Glasser et al. 2016). Additionally, task fMRI contrasts from nine tasks were also employed to infer areal boundaries (Barch et al. 2013), which were chosen to optimally balance breadth vs depth and scan time (Elam et al. 2021). Although we regard the MMP1 as a step change in our understanding of brain organization, and in particular of the fine-grained organization and structure of the PFC both in humans and in non-human primates (Donahue et al. 2018), we would like to suggest that more information gathered from task-based fMRI will be needed to better understand the functional subdivision of the pPFC. In particular, following the taxonomy proposed by the MMP1, major efforts should be made to isolate FEF activity from posterior activity in the premotor cortex on the one hand (area 6d), and from a newly discovered language selective region that borders the FEF ventrally on the other, namely area 55b (for a discussion on inter-individual variability in the spatial organization of these regions see Glasser et al. 2016). Ultimately, future developments of a functional localization method will facilitate the convergence of atlas-based and fMRI information to allow delineating anatomical clusters of activation within FEF with adequate functional specificity. Our ALE results partly suggest that this is needed as the current gold standard for localizing the FEF may actually lead to the inclusion of voxels from heterogeneous brain regions as defined according to the MMP1 atlas, possibly also due to the greater inter-subject variability that characterize the pPFC (Bedini and Baldauf 2021; Glasser et al. 2016). In this direction, a very compelling set of results were reported by Mackey et al. (2017), who identified two retinotopic maps in the sPCS (sPCS1 and SPC2) and a third one in the iPCS. By examining the correspondences between their results and the MMP1 (see Figure 8 from their study), they found that the sPCS2 corresponded to the FEF, while the sPCS1 corresponded to areas 6a and 6d. Interestingly, they also reported that in all subjects and in both hemispheres, the foveal representation was localized in the fundus of the sPCS, at its intersection with the SFS. This description closely matches the localization of our ALE peaks across experiments, which raises the question of whether the fMRI contrasts we included in our meta-analysis could be targeting specific neural populations within the FEF. It is well established that in the macaque, a population of neurons shows increased firing rates when the animal is fixating and is inhibited when executing saccades (hence termed ‘fixation’ neurons; Bruce and Golberg 1985; Hanes et al. 1998; Lowe and Schall 2018). Are these populations of neurons also present in humans, and how are they distributed within the FEF? Are these neurons associated with the significant increase in the BOLD signal when comparing saccades to peripheral positions against a



fixation baseline, and what is the role of saccadic amplitude in isolating peaks of activity within the FEF (see Grosbras 2016)?

To further examine the role of different fMRI contrasts in the localization of the FEF, in three control analyses, we systematically investigated the presence of additional activations along the banks of the sPCS and iPCS, and of segregated clusters of activity for prosaccades > fixation vs antisaccades > prosaccades and prosaccades > fixation vs valid > neutral/invalid trials in covert spatial attention tasks. In the first control analysis, we showed that by using a less conservative multiple comparison correction method (i.e., cluster-level FWE), we could uncover iFEF activations in both hemispheres. These covered the dorsal most part of the iPCS and extended to the posterior premotor cortex. This highlights the fact that, although these clusters may be under-reported in the literature (Derrfuss et al. 2012), they were nevertheless consistently activated in our sample of experiments. While the analysis of prosaccades > fixation vs antisaccades > prosaccades suggested segregated clusters of activity in the anterior-dorsal sPCS/SFS for antisaccades, replicating previous results (Cieslik et al. 2016), the region of overlap was again localized at the junction of the sPCS with the SFS. Compared to the main localizer sample (where we also included antisaccades > fixation, and antisaccades & prosaccades > fixation contrast), pure prosaccades > fixation contrasts revealed two distinct ALE peaks in the right hemisphere, suggesting a higher variability along the lateral axis. Finally, by comparing prosaccades > fixation vs valid > neutral/invalid trials contrasts (see Supplementary Figure 3), we found overlapping activations near the junction of the sPCS and SFS, as expected from previous studies (Astafiev et al. 2003; Corbetta et al. 1998; de Haan et al. 2008), suggesting that if anything, covert spatial attention paradigms may be equally adept as FEF functional localizers compared to the current gold standard, although more trials may be needed to reliably elicit activations in all subjects due to the weaker nature of the signal measured (Beauchamp et al. 2001; De Haan et al. 2008). An additional aspect that may be worth investigating is whether one or more of these clusters (for example, the iFEF) are dependent on some artifacts present in the experimental design or analysis. In the 35 experiments we analyzed, 10 didn't record eye movements in the scanner (see Table 1), making it at least likely that some of these clusters were driven by mixed signals and in the worst case, by spurious neural activity that was not related to saccadic behavior. For example, it is well documented that eye blinks can contaminate BOLD signal (Bristow et al. 2005; Hupé et al. 2012), and this fact was invoked to explain discrepancies in the oculomotor organization in primates (Tehovnik et al. 2000) and as a signal driving iFEF responses (Amiez and Petrides 2009; Kato and Miyauchi 2003). Hence, we very much agree with the caveat that the way the FEF is defined is ultimately constrained by the technique employed (Schall et al. 2020; Vernet et al. 2014), and in particular its spatial resolution. The localization and the extent of the FEF cluster should be inferred based on the convergence of multiple criteria (primarily architectonic, sulcal, functional, connectional, and also comparative), some of which may not be available due to lack of time, equipment and resources. With the present ALE meta-analysis, we aimed at providing updated quantitative evidence on the localization of this region in standard space using typical functional localizers across over 400 subjects, but more efforts will be needed to understand the organization of the human eye fields in the pPFC and their relationship with sulcal neuroanatomy at the individual-subject level (Amiez et al. 2006; Amiez and Petrides 2018; Frost and Goebel 2012). Careful mapping of the localization of the human FEF is essential to bridge research in humans and non-human primates, and

could be for example extremely important for testing hypotheses of homologies across species based on connectivity information (Mars et al. 2021; Neggers et al. 2015; Sallet et al. 2013).

The study of the role of the ventrolateral PFC in various cognitive functions such as non-spatial attention, working memory and cognitive control made enormous progress with the advent of fMRI (Cole and Schneider 2007; Courtney et al. 1998; Duncan 2010; Owen et al. 1998), and led to the definition of the IFJ as a separate brain region involved in critical aspects of all these functions (Brass et al. 2005; Derrfuss et al. 2004, 2005). This region seems to be tightly coupled with specific sulcal landmarks across individuals, namely the junction of the iPCS and the IFS (Derrfuss et al. 2009; Juch et al. 2005), and plays a crucial role in the fronto-parietal network (Cole and Schneider 2007; Cole et al. 2013; Yeo et al. 2011). In line with these results, a recent fMRI study in a large number of subjects showed that the IFJp belongs to the core multiple demand system of the brain (Assem et al. 2020). A subsequent study found that thanks to improved inter-subject alignment techniques (i.e., multi-modal surface matching; Robinson et al. 2018), working memory load effects were localized in this region across subjects and visual and auditory modalities (Assem et al. 2021). Even though these results indicate that this region is sensitive to manipulations that involve task difficulty and that it may not be selective to a single sensory modality (i.e., vision) when working memory load is increased, there are on the other hand strong indications that activity patterns in the IFJ are consistently selective to non-spatial information across paradigms (Bedini and Baldauf 2021). In this study, we therefore pooled together results from the various tasks that have been used to localize this region (see Table 4) spanning from attentional (i.e., RSVP/oddball; Asplund et al. 2010; and endogenous cueing paradigms; see for example Baldauf and Desimone 2014; Zhang et al. 2018), working memory (primarily n-back paradigms; Zanto et al. 2010), and cognitive control paradigms (i.e., task-switching and Stroop tasks; Brass and Von Cramon 2002; Derrfuss et al. 2010). Following previous results (Derrfuss et al. 2005), we reasoned that the spatial convergence across these paradigms (rather than a single contrast) would allow us to infer the accurate localization of the IFJ in standard space. Consistent with our hypothesis, we found two prominent clusters of activation in the ventral PFC. Based on the respective ALE peak values, the highest convergence was found in the posterior bank of the iPCS, approximately at the height of its ventral junction with the IFS (see Figure 3; Table 2). The LH IFJ ALE peak lies in BA 6, whereas the RH IFJ peak lies within BA 9. The distinctive architecture of the IFJ remains elusive, but these peaks agree with the general idea that this area is localized in several Brodmann areas (BA6, 8, 9, 44 and 45), and may correspond to a specific cyto- and chemo-architecture found dorsal to BA44 (Amunts and Von Cramon 2006; for a recent fine-grained analysis of its architecture see Ruland et al. 2022). The coordinates of these peaks were virtually identical to those reported in Derrfuss et al. (2005), although the RH IFJ seemed to be slightly more ventral compared to their results. Macro-anatomically, the LH IFJ peak was localized within the precentral gyrus, and the RH IFJ peak was localized in the pars opercularis. The comparison of these results with the MMP1 (Glasser et al. 2016) through their projection to the FSaverage surface revealed additional interesting spatial patterns. Both IFJ clusters spanned several regions of the MMP1, including areas PEF, 6r, IFJp and IFJa (Figure 6 panel B), with the majority of the voxels being localized around the borders of IFJp, 6r and the PEF. Moreover, both ALE peaks were localized in area 6r, ventral to the IFJp. As previously discussed in relation to the FEF ALE results, these results suggest that the paradigms currently employed to localize the IFJ may actually lead to the inclusion of voxels from heterogeneous brain regions as defined according to this atlas. This problem is further

exacerbated by the fact that the IFJ itself and the neighboring regions are also part of the multiple demand system, so many experimental manipulations will tend to coactivate some of them at the same time, thus concealing its boundaries.

We therefore also examined potential differences in localization between paradigms in a control analysis. Taken together, our results showed that oddball/cueing paradigms tend to activate voxels that are localized in the posterior aspect of the IFS, whereas both working memory and cognitive control paradigms tend to activate more posterior voxels in the banks of the iPCS. Based on these results we would like to offer some suggestions on how to effectively localize the IFJ and segregate it from adjacent brain regions. First of all, at the general level, contrasts involving two demanding experimental conditions (e.g., task switch > repeat trials) may be more appropriate to measure activity within the IFJ compared to experimental trials vs passive fixation conditions. Secondly, an even more stringent way to isolate this region would be to compare experimental conditions that are matched in difficulty, thus avoiding contamination from non-specific load effects (Baldauf and Desimone 2014). In our included paradigms, oddball paradigms usually contrast activity between oddball and target trials, leading however to a low number of trials that are used as functional localizers within each run as a result (Han and Marois 2014). An additional problem may be caused by spatial smoothing, which would lead to merging activity with the IFG, a node classically viewed as belonging to the ventral attention network (Corbetta and Shulman 2002), which is also significantly activated in these paradigms (Levy and Wagner 2011). Therefore, a more straightforward way to isolate the IFJ from the IFG may be achieved by administering top-down feature- and object-based attention tasks (Baldauf and Desimone 2014; Liu et al. 2011; Liu 2016; Zhang et al. 2018) and contrasting valid > invalid trials collapsed across the stimuli features/dimensions (e.g., similarly to the approach reported in Zanto et al. 2010). Posteriorly, another important issue is how to segregate IFJ activity from the PEF (or the iFEF). Derrfuss et al. (2012) reported that by employing a Stroop paradigm and contrasting incongruent > congruent trials, they were able to isolate activity from the adjacent iFEF (which was activated by the execution of voluntary saccades in darkness) in the native space in all the subjects they analyzed (Derrfuss et al. 2012). These results show a promising way to infer the posterior IFJ functional border. As suggested previously, the presence of significant voxels within the iFEF in our results is difficult to interpret given that, in our IFJ sample, only two out of 32 experiments (see Table 2) employed strict monitoring of eye movements in the scanner. The possibility that the convergence in iFEF in this sample may be due to this confound cannot be therefore completely ruled out (Amiez and Petrides 2009; Kato and Miyauchi 2003). An interesting approach that recognizes the integrative nature of the IFJ draws from the combination of different paradigms and the conjunction of the associated activity to localize this region, which may overcome some of the previous limitations. The study by Stiers and Goulas (2018) analyzed the voxel responses across three different tasks (Eriksen flanker task, backmatching or n-back task, and a response switching task) to define the prefrontal nodes of the multiple demand system in 12 subjects. A manipulation of task difficulty in each of the previous tasks was used to identify voxels that were modulated by increasing cognitive demands, which were used to define ROIs in each subject in a conjunction analysis across tasks for further analyzing their relative task preference and functional connectivity patterns. Their conjunction analysis revealed local maxima of activity within the IFJ (see Figure 2 in Stiers and Goulas 2018), where voxels with different task preferences exhibited distinct functional connectivity patterns with the rest of the brain (see Figure 7 of the same study). Based on these results, it may be

argued that no single task alone would adequately capture the selectivity patterns of neural populations within the IFJ; rather, manipulations of task difficulty combined with the administration of different tasks could provide an unbiased way of localizing this region in individual participants. The results of the present study aimed at providing quantitative evidence of the convergence of activations within the IFJ across non-spatial attentional, working memory, and cognitive control tasks across over 500 subjects, which we hope will help guide future research aimed at understanding the relationship between the function and localization of the IFJ, and its relationship with sulcal neuroanatomy at the individual subject level (Derrfuss et al. 2009).

A secondary goal of the present study was to uncover the task-based functional connectivity fingerprint (Passingham et al. 2002) of the FEF and the IFJ in a fully data-driven fashion. We retrieved in the BrainMap database all the studies that reported activations within a cuboid seed centered around the FEF and IFJ standard coordinates found in our ALE main localizer analyses and we employed the MACM technique (Langner and Camilleri 2021) to uncover their coactivation profiles. Importantly, while previous studies already performed MACM analyses on the FEF (Cieslik et al. 2016) and the IFJ (Muhle-Karbe et al. 2016; Sundermann and Pfliegerer 2012), our study is to our knowledge the first that used this technique on the results of an independent localizer ALE analysis of these regions (and not a manual or atlas-based delineation) using a conservative seed extent (6 mm). Our MACM analysis allowed adequately powered inference in each seed region ( $n > 19$  experiments; Eickhoff et al. 2016) and revealed broad networks of coactivations that encompassed the frontal, parietal and temporal cortices (see Figure 7). The most remarkable differences between FEF and IFJ coactivation patterns were that on the one hand, the LH and RH FEF coactivated with the bilateral ventrolateral PFC (iFEF and IFJ), whereas only the LH IFJ coactivated with the left FEF in the experiments retrieved. On the other hand, the LH IFJ had stronger and more widespread coactivations in PFC and in the insular cortex and also coactivated with the inferotemporal cortex. These coactivation patterns may be essential for the IFJ to perform its role in feature- and object-based attention tasks (Baldauf and Desimone 2014) and could be in turn supported by its underlying anatomical connectivity (Baldauf and Desimone 2014; Bedini et al. 2021). These results are consistent with the idea of a dorso-ventral segregation of fronto-parietal coactivations forming a spatial/motor and a non-spatial/motor network, and that are in turn associated with the first and third branch of the superior longitudinal fasciculus, respectively (Parlatini et al. 2017). While the LH and RH FEF coactivation patterns were largely symmetrical, there were some interesting asymmetries between LH and RH IFJ coactivations. Specifically, considering the respective seed's ipsilateral hemisphere, the LH IFJ had coactivations with the FEF and the inferotemporal cortex, whereas the RH IFJ lacked those. This potentially hints at the distinctive role of the LH IFJ that may reflect its involvement in a lateralized language network (Ji et al. 2019). In addition, the functional decoding of these coactivation patterns highlighted the behavioral domains that were significantly associated with the activity of the FEF and IFJ seeds (see MACM results). FEF coactivations were globally more associated with the action.execution and cognition.attention sub-domains, while IFJ coactivations were significantly associated with a larger number of behavioral domains ranging from cognition (attention, working memory, and language), perception (vision and audition), as well as action (execution and inhibition). These results suggest that these systematic coactivation patterns allow these regions to support multiple specialized roles in flexible goal-driven behavior (particularly in the case of the IFJ, as they further highlight its role in the multiple demand system; Assem et al. 2020).

In conclusion, our study reveals the spatial organization and accurate localization of two regions localized in the posterior lateral PFC, namely the FEF and the IFJ. These regions are tightly linked to sulcal landmarks as measured using fMRI across hundreds of subjects, with the FEF being localized at the junction of the sPCS and the SFS, and the IFJ at the junction of the iPCS and the IFS. Functionally, they appear to be organized according to a dorso-ventral gradient, going from areas responsible for sensorimotor transformations and action execution (FEF, iFEF), to areas that are involved in maintaining and updating behavioral goals according to internal representations (IFJ; Nee et al. 2013; O'Reilly 2010). Taken together, our findings aim at proposing a consensus standard localization of these regions in standard space, and meta-analytic groundwork to investigate the relationship between functional specialization and connectivity in large publicly available neuroimaging datasets and databases (e.g., Markiewicz et al. 2021; Van Essen et al. 2013), as well as to guide future non-invasive brain stimulation studies.

## Funding

This work was supported by a doctoral scholarship awarded to MB financed by the University of Trento (Center for Mind/Brain Sciences).

## Competing Interests

The authors have no relevant financial or non-financial interests to disclose.

## Author contributions

Conceptualization: **MB, DB**; Methodology: **MB, EO, PA, DB**; Software: **MB**; Validation: **MB**; Formal analysis: **MB**; Investigation: **MB**; Resources: **MB, DB**; Data curation: **MB**; Writing - original draft: **MB**; Writing - review and editing: **MB, EO, PA, DB**; Visualization: **MB**; Supervision: **EO, PA, DB**; Project administration: **MB**; Funding acquisition: **MB**.

## Data availability

The authors are committed to making the datasets generated during the current study available in a Neurovault repository upon article acceptance.



## Acknowledgments

We would like to thank Luca Turella and Daniel Adams for their comments on the preliminary results of this study. We would also like to thank Gabriele Amorosino and Francesca Saviola for technical advice, and Vittorio Iacovella and Giorgio Marinato for their advice on resource/data sharing.

## References

- Abdollahi RO, Kolster H, Glasser MF, et al (2014) Correspondences between retinotopic areas and myelin maps in human visual cortex. *Neuroimage* 99:509–524. <https://doi.org/10.1016/j.neuroimage.2014.06.042>
- Alkan Y, Biswal BB, Alvarez TL (2011) Differentiation between vergence and saccadic functional activity within the human frontal eye fields and midbrain revealed through fMRI. *PLoS One* 6:1-14. <https://doi.org/10.1371/journal.pone.0025866>
- Amiez C, Kostopoulos P, Champod AS, Petrides M (2006) Local morphology predicts functional organization of the dorsal premotor region in the human brain. *J Neurosci* 26:2724–2731. <https://doi.org/10.1523/JNEUROSCI.4739-05.2006>
- Amiez C, Petrides M (2009) Anatomical organization of the eye fields in the human and non-human primate frontal cortex. *Prog Neurobiol* 89:220–30. <https://doi.org/10.1016/j.pneurobio.2009.07.010>
- Amiez C, Petrides M (2018) Functional rostro-caudal gradient in the human posterior lateral frontal cortex. *Brain Struct Funct* 223:1487–1499. <https://doi.org/10.1007/s00429-017-1567-z>
- Amunts K, Cramon DY Von (2006) Special Issue : Position Paper the Anatomical Segregation of the Frontal Cortex : What Does It Mean for Function ? *Brain* 3:525–528. [https://doi.org/10.1016/S0010-9452\(08\)70392-7](https://doi.org/10.1016/S0010-9452(08)70392-7)
- Amunts K, Mohlberg H, Bludau S, Zilles K (2020) Julich-Brain: A 3D probabilistic atlas of the human brain's cytoarchitecture. *Science* 369:988–992. <https://doi.org/10.1126/science.abb4588>
- Amunts K, Zilles K (2015) Architectonic Mapping of the Human Brain beyond Brodmann. *Neuron* 88:1086–1107. <https://doi.org/10.1016/j.neuron.2015.12.001>
- Armbruster DJN, Ueltzhöffer K, Basten U, Fiebach CJ (2012) Prefrontal cortical mechanisms underlying individual differences in cognitive flexibility and stability. *J Cogn Neurosci* 24:2385–2399. [https://doi.org/10.1162/jocn\\_a\\_00286](https://doi.org/10.1162/jocn_a_00286)
- Astafiev S., Shulman GL, Stanley CM, et al (2003). Functional organization of human intraparietal and frontal cortex for attending, looking, and pointing. *J Neurosci* 23:4689-4699. <https://doi.org/10.1523/JNEUROSCI.23-11-04689.2003>
- Atmaca S, Stadler W, Keitel A, et al (2013) Prediction processes during multiple object tracking (MOT): Involvement of dorsal and ventral premotor cortices. *Brain Behav* 3:683–700. <https://doi.org/10.1002/brb3.180>
- Asplund CL, Todd JJ, Snyder AP, Marois R (2010) A central role for the lateral prefrontal cortex in goal-directed and stimulus-driven attention. *Nat Neurosci* 13:507–512. <https://doi.org/10.1038/nn.2509>
- Assem M, Glasser MF, Van Essen DC, Duncan J (2020) A Domain-General Cognitive Core Defined in Multimodally Parcellated Human Cortex. *Cereb Cortex* 1–20. <https://doi.org/10.1093/cercor/bhaa023>
- Assem M, Shashidhara S, Glasser MF, Duncan J (2021) Precise Topology of Adjacent Domain-General and Sensory-Biased Regions in the Human Brain. *Cereb Cortex* 1–17. <https://doi.org/10.1093/cercor/bhab362>

- Baldauf D, Desimone R (2014) Neural mechanisms of object-based attention. *Science* 344: 424–427. <https://doi.org/10.1126/science.1247003>
- Bär S, Hauf M, Barton JJS, Abegg M (2016) The neural network of saccadic foreknowledge. *Exp Brain Res* 234:409–418. <https://doi.org/10.1007/s00221-015-4468-5>
- Barch DM, Burgess GC, Harms MP, et al (2013) Function in the human connectome: Task-fMRI and individual differences in behavior. *Neuroimage* 80:169–189. <https://doi.org/10.1016/j.neuroimage.2013.05.033>
- Beauchamp MS, Petit L, Ellmore TM, et al (2001) A parametric fMRI study of overt and covert shifts of visuospatial attention. *Neuroimage* 14:310–321. <https://doi.org/10.1006/nimg.2001.0788>
- Bedini M, Baldauf D (2021) Structure, function and connectivity fingerprints of the frontal eye field versus the inferior frontal junction: A comprehensive comparison. *Eur J Neurosci* 54:5462–5506. <https://doi.org/10.1111/ejn.15393>
- Bedini M, Olivetti E, Avesani, P & Baldauf D (2021). The anatomical pathways underlying spatial versus non-spatial attention. *Cogn Process* 22 (Suppl 1):S35. In Jeffery K (2021) Abstracts and authors of the 8th International Conference on Spatial Cognition: Cognition and Action in a Plurality of Spaces (ICSC 2021). <https://doi.org/10.1007/s10339-021-01058-x>
- Benson NC, Butt OH, Datta R, et al (2012) The retinotopic organization of striate cortex is well predicted by surface topology. *Curr Biol* 22:2081–2085. <https://doi.org/10.1016/j.cub.2012.09.014>
- Berman RA, Colby CL, Genovese CR, et al (1999) Cortical networks subserving pursuit and saccadic eye movements in humans: An FMRI study. *Hum Brain Mapp* 8:209–225. [https://doi.org/10.1002/\(SICI\)1097-0193\(1999\)8:4<209::AID-HBM5>3.0.CO;2-0](https://doi.org/10.1002/(SICI)1097-0193(1999)8:4<209::AID-HBM5>3.0.CO;2-0)
- Bichot NP, Heard MT, DeGennaro EM, Desimone R (2015) A Source for Feature-Based Attention in the Prefrontal Cortex. *Neuron* 88:832–844. <https://doi.org/10.1016/j.neuron.2015.10.001>
- Bichot NP, Xu R, Ghadooshahy A, et al (2019) The role of prefrontal cortex in the control of feature attention in area V4. *Nat Commun* 10:1–12. <https://doi.org/10.1038/s41467-019-13761-7>
- Blanke O, Spinelli CAL, Thut G, et al (2000) Location of the human frontal eye field as defined by electrical cortical stimulation: anatomical, functional and electrophysiological characteristics. *NeuroReport* 11:1907–1913. <https://doi.org/10.1097/00001756-200006260-00021>
- Bode S, Haynes JD (2009) Decoding sequential stages of task preparation in the human brain. *Neuroimage* 45:606–613. <https://doi.org/10.1016/j.neuroimage.2008.11.031>
- Bollinger J, Rubens MT, Zanto TP, Gazzaley A (2010) Expectation-driven changes in cortical functional connectivity influence working memory and long-term memory performance. *J Neurosci* 30:14399–14410. <https://doi.org/10.1523/JNEUROSCI.1547-10.2010>
- Botvinik-Nezer R, Holzmeister F, Camerer CF, et al (2020) Variability in the analysis of a single neuroimaging dataset by many teams. *Nature* 582:84–88. <https://doi.org/10.1038/s41586-020-2314-9>
- Braga RM, Fu RZ, Seemungal BM, et al (2016) Eye movements during auditory attention predict individual differences in dorsal attention network activity. *Front Hum Neurosci* 10:1–13. <https://doi.org/10.3389/fnhum.2016.00164>
- Brass, M., Derrfuss, J., Forstmann, B., & von Cramon, D. Y. (2005). The role of the inferior frontal junction area in cognitive control. *Trends Cogn Sci* 9:314-316. <https://doi.org/10.1016/j.tics.2005.05.001>
- Brass M, Von Cramon DY (2002) The role of the frontal cortex in task preparation. *Cereb Cortex* 12:908–914. <https://doi.org/10.1093/cercor/12.9.908>
- Brass M, Von Cramon DY (2004) Decomposing components of task preparation with functional magnetic resonance imaging. *J Cogn Neurosci* 16:609–620. <https://doi.org/10.1162/089892904323057335>

- Brett M, Johnsrude IS, Owen AM (2002) The problem of functional localization in the human brain. *Nat Rev Neurosci* 3:243–249. <https://doi.org/10.1038/nrn756>
- Bristow D, Haynes JD, Sylvester R, et al (2005) Blinking suppresses the neural response to unchanging retinal stimulation. *Curr Biol* 15:1296–1300. <https://doi.org/10.1016/j.cub.2005.06.025>
- Brodman K, (1909) Vergleichende Lokalisationslehre der Grosshirnrinde in ihren Prinzipien dargestellt auf Grund des Zellenbaues. Barth.
- Brown MRG, Goltz HC, Vilis T, et al (2006) Inhibition and generation of saccades: Rapid event-related fMRI of prosaccades, antisaccades, and nogo trials. *Neuroimage* 33:644–659. <https://doi.org/10.1016/j.neuroimage.2006.07.002>
- Bruce CJ, Goldberg ME (1985) Primate frontal eye fields. I. Single neurons discharging before saccades. *J Neurophysiol* 53:603–635. <https://doi.org/10.1152/jn.1985.53.3.603>
- Bruce CJ, Goldberg ME, Bushnell MC, Stanton GB (1985) Primate frontal eye fields. II. Physiological and anatomical correlates of electrically evoked eye movements. *J Neurophysiol* 54:714–734. <https://doi.org/10.1152/jn.1985.54.3.714>
- Buschman TJ, Miller EK (2009) Serial, Covert Shifts of Attention during Visual Search Are Reflected by the Frontal Eye Fields and Correlated with Population Oscillations. *Neuron* 63:386–396. <https://doi.org/10.1016/j.neuron.2009.06.020>
- Carrasco M (2011) Visual attention: The past 25 years. *Vision Res* 51:1484–1525. <https://doi.org/10.1016/j.visres.2011.04.012>
- Chen Z, Lei X, Ding C, et al (2013) The neural mechanisms of semantic and response conflicts: An fMRI study of practice-related effects in the Stroop task. *Neuroimage* 66:577–584. <https://doi.org/10.1016/j.neuroimage.2012.10.028>
- Cieslik EC, Seidler I, Laird AR, et al (2016) Different involvement of subregions within dorsal premotor and medial frontal cortex for pro- and antisaccades. *Neurosci Biobehav Rev* 68:256–269. <https://doi.org/10.1016/j.neubiorev.2016.05.012>
- Coalson TS, Van Essen DC, Glasser MF (2018) The impact of traditional neuroimaging methods on the spatial localization of cortical areas. *Proc Natl Acad Sci U S A* 115:E6356–E6365. <https://doi.org/10.1073/pnas.1801582115>
- Cole MW, Schneider W (2007) The cognitive control network: Integrated cortical regions with dissociable functions. *Neuroimage* 37:343–360. <https://doi.org/10.1016/j.neuroimage.2007.03.071>
- Cole MW, Reynolds JR, Power JD, et al (2013) Multi-task connectivity reveals flexible hubs for adaptive task control. *Nat Neurosci* 16:1348–1355. <https://doi.org/10.1038/nn.3470>
- Connolly JD, Goodale MA, Desouza JFX, et al (2000) A comparison of frontoparietal fMRI activation during anti-saccades and anti-pointing. *J Neurophysiol* 84:1645–1655. <https://doi.org/10.1152/jn.2000.84.3.1645>
- Connolly JD, Goodale MA, Menon RS, Munoz DP (2002) Human fMRI evidence for the neural correlates of preparatory set. *Nat Neurosci* 5:1345–1352. <https://doi.org/10.1038/nn969>
- Connolly JD, Goodale MA, Goltz HC, Munoz DP (2005) fMRI activation in the human frontal eye field is correlated with saccadic reaction time. *J Neurophysiol* 94:605–611. <https://doi.org/10.1152/jn.00830.2004>
- Connolly JD, Goodale MA, Cant JS, Munoz DP (2007) Effector-specific fields for motor preparation in the human frontal cortex. *Neuroimage* 34:1209–1219. <https://doi.org/10.1016/j.neuroimage.2006.10.001>

- Corbetta M, Akbudak E, Conturo TE, et al (1998) A common network of functional areas for attention and eye movements. *Neuron* 21:761–773. [https://doi.org/10.1016/S0896-6273\(00\)80593-0](https://doi.org/10.1016/S0896-6273(00)80593-0)
- Corbetta M, Shulman GL (2002) Control of goal-directed and stimulus-driven attention in the brain. *Nat Rev Neurosci* 3:201–215. <https://doi.org/10.1038/nrn755>
- Corradi-Dell'Acqua C, Fink GR, Weidner R (2015) Selecting category specific visual information: Top-down and bottom-up control of object based attention. *Conscious Cogn* 35:330–341. <https://doi.org/10.1016/j.concog.2015.02.006>
- Courtney SM, Petit L, Maisog JM, et al (1998) An area specialized for spatial working memory in human frontal cortex. *Science* 279:1347–1351. <https://doi.org/10.1126/science.279.5355.1347>
- Christophel TB, Allefeld C, Endisch C, Haynes JD (2018) View-Independent Working Memory Representations of Artificial Shapes in Prefrontal and Posterior Regions of the Human Brain. *Cereb Cortex* 28:2146–2161. <https://doi.org/10.1093/cercor/bhx119>
- Curtis CE, D'Esposito M (2003) Success and failure suppressing reflexive behavior. *J Cogn Neurosci* 15:409–418. <https://doi.org/10.1162/089892903321593126>
- Curtis CE, Connolly JD (2008) Saccade preparation signals in the human frontal and parietal cortices. *J Neurophysiol* 99:133–145. <https://doi.org/10.1152/jn.00899.2007>
- de Haan B, Morgan PS, Rorden C (2008) Covert orienting of attention and overt eye movements activate identical brain regions. *Brain Res* 1204:102–111. <https://doi.org/10.1016/j.brainres.2008.01.105>
- De Pasquale F, Della Penna S, Snyder AZ, et al (2010) Temporal dynamics of spontaneous MEG activity in brain networks. *Proc Natl Acad Sci U S A* 107:6040–6045. <https://doi.org/10.1073/pnas.0913863107>
- Derrfuss J, Brass M, Neumann J, Von Cramon DY (2005) Involvement of the inferior frontal junction in cognitive control: Meta-analyses of switching and stroop studies. *Hum Brain Mapp* 25:22–34. <https://doi.org/10.1002/hbm.20127>
- Derrfuss J, Brass M, Yves Von Cramon D (2004) Cognitive control in the posterior frontolateral cortex: Evidence from common activations in task coordination, interference control, and working memory. *Neuroimage* 23:604–612. <https://doi.org/10.1016/j.neuroimage.2004.06.007>
- Derrfuss J, Brass M, Von Cramon DY, et al (2009) Neural activations at the junction of the inferior frontal sulcus and the inferior precentral sulcus: Interindividual variability, reliability, and association with sulcal morphology. *Hum Brain Mapp* 30:299–311. <https://doi.org/10.1002/hbm.20501>
- Derrfuss J, Vogt VL, Fiebach CJ, et al (2012) Functional organization of the left inferior precentral sulcus: Dissociating the inferior frontal eye field and the inferior frontal junction. *Neuroimage* 59:3829–3837. <https://doi.org/10.1016/j.neuroimage.2011.11.051>
- Desikan RS, Ségonne F, Fischl B, et al (2006) An automated labeling system for subdividing the human cerebral cortex on MRI scans into gyral based regions of interest. *Neuroimage* 31:968–980 <https://doi.org/10.1016/j.neuroimage.2006.01.021>
- DeSouza JFX, Everling S (2002) Neural correlates for preparatory set associated with pro-saccades and anti-saccades in humans investigated with event-related fMRI. *J Vis* 2:1016–1023. <https://doi.org/10.1167/2.7.578>
- Destrieux C, Fischl B, Dale A, Halgren E (2010) Automatic parcellation of human cortical gyri and sulci using standard anatomical nomenclature. *Neuroimage* 53:1–15. <https://doi.org/10.1016/j.neuroimage.2010.06.010>
- Donahue CJ, Glasser MF, Preuss TM, et al (2018) Quantitative assessment of prefrontal cortex in humans relative to nonhuman primates. *Proc Natl Acad Sci U S A* 115:E5183–E5192. <https://doi.org/10.1073/pnas.1721653115>

Duecker F, Formisano E, Sack AT (2013) Hemispheric differences in the voluntary control of spatial attention: Direct evidence for a right-hemispheric dominance within frontal cortex. *J Cogn Neurosci* 25:1332–1342. [https://doi.org/10.1162/jocn\\_a\\_00402](https://doi.org/10.1162/jocn_a_00402)

Duncan J (2010) The multiple-demand (MD) system of the primate brain: mental programs for intelligent behaviour. *Trends Cogn Sci* 14:172–179. <https://doi.org/10.1016/j.tics.2010.01.004>

Eickhoff SB, Bzdok D, Laird AR, Kurth F, Fox PT (2012) Activation likelihood estimation meta-analysis revisited. *Neuroimage* 59:2349–2361. <https://doi.org/10.1016/j.neuroimage.2011.09.017>

Eickhoff SB, Laird AR, Fox PM, et al (2017) Implementation errors in the GingerALE Software: Description and recommendations. *Hum Brain Mapp* 38:7–11. <https://doi.org/10.1002/hbm.23342>

Eickhoff SB, Laird AR, Grefkes C, et al (2009) Coordinate-Based Activation Likelihood Estimation Meta-Analysis of Neuroimaging Data : A Random-Effects Approach Based on Empirical Estimates of Spatial Uncertainty. *Hum Brain Mapp* 29:2907–2926. <https://doi.org/10.1002/hbm.20718>

Eickhoff SB, Nichols TE, Laird AR, et al (2016) Behavior, sensitivity, and power of activation likelihood estimation characterized by massive empirical simulation. *Neuroimage* 137:70–85. <https://doi.org/10.1016/j.neuroimage.2016.04.072>

Eickhoff SB, Yeo BTT, Genov S (2018) Imaging-based parcellations of the human brain. *Nat Rev Neurosci* 19:672–686. <https://doi.org/10.1038/s41583-018-0071-7>

Elam JS, Glasser MF, Harms MP, et al (2021) The Human Connectome Project: A retrospective. *Neuroimage* 244:118543. <https://doi.org/10.1016/j.neuroimage.2021.118543>

Fedorenko E (2021) The early origins and the growing popularity of the individual-subject analytic approach in human neuroscience. *Curr Opin Behav Sci* 40:105–112. <https://doi.org/10.1016/j.cobeha.2021.02.023>

Felleman DJ, Van Essen DC (1991) Distributed hierarchical processing in the primate cerebral cortex. *Cereb Cortex* 1:1–47. <https://doi.org/10.1093/cercor/1.1.1-a>

Fernandez-Ruiz J, Peltsch A, Alahyane N, et al (2018) Age related prefrontal compensatory mechanisms for inhibitory control in the antisaccade task. *Neuroimage* 165:92–101. <https://doi.org/10.1016/j.neuroimage.2017.10.001>

Fiebelkorn IC, Kastner S (2020) Functional Specialization in the Attention Network. *Annu Rev Psychol* 71:1–29. <https://doi.org/10.1146/annurev-psych-010418-103429>

Fischl B, Sereno MI, Tootell RBH, Dale AM (1999) High-resolution intersubject averaging and a coordinate system for the cortical surface. *Hum Brain Mapp* 8:272–284. [https://doi.org/10.1002/\(SICI\)1097-0193\(1999\)8:4<272::AID-HBM10>3.0.CO;2-4](https://doi.org/10.1002/(SICI)1097-0193(1999)8:4<272::AID-HBM10>3.0.CO;2-4)

Fischl B, Rajendran N, Busa E, et al (2008) Cortical folding patterns and predicting cytoarchitecture. *Cereb Cortex* 18:1973–1980. <https://doi.org/10.1093/cercor/bhm225>

Fonov V, Evans A, McKinstry R, et al (2009) Unbiased nonlinear average age-appropriate brain templates from birth to adulthood. *Neuroimage* 47:S102. [https://doi.org/10.1016/s1053-8119\(09\)70884-5](https://doi.org/10.1016/s1053-8119(09)70884-5)

Fox MD, Corbetta M, Snyder AZ, et al (2006) Spontaneous neuronal activity distinguishes human dorsal and ventral attention systems. *Proc Natl Acad Sci U S A* 103:10046–10051. <https://doi.org/10.1073/pnas.0604187103>

Fox PT, Laird AR, Fox SP, et al (2005) BrainMap taxonomy of experimental design: Description and evaluation. *Hum Brain Mapp* 25:185–198. <https://doi.org/10.1002/hbm.20141>

Fox PT, Lancaster JL (2002) Mapping context and content: The BrainMap model. *Nat Rev Neurosci* 3:319–321. <https://doi.org/10.1038/nrn789>



Fox PT, Lancaster JL, Laird AR, Eickhoff SB (2014) Meta-analysis in human neuroimaging: Computational modeling of large-scale databases. *Annu Rev Neurosci* 37:409–434. <https://doi.org/10.1146/annurev-neuro-062012-170320>

Fransson P, Flodin P, Seimyr GÖ, Pansell T (2014) Slow fluctuations in eye position and resting-state functional magnetic resonance imaging brain activity during visual fixation. *Eur J Neurosci* 40:3828–3835. <https://doi.org/10.1111/ejn.12745>

Frost MA, Goebel R (2012) Measuring structural – functional correspondence : Spatial variability of specialised brain regions after macro-anatomical alignment. *Neuroimage* 59:1369–1381. <https://doi.org/10.1016/j.neuroimage.2011.08.035>

Furlan M, Smith AT, Walker R (2016) An fMRI investigation of preparatory set in the human cerebral cortex and superior colliculus for pro- and anti-saccades. *PLoS One* 11:1–25. <https://doi.org/10.1371/journal.pone.0158337>

Fuster JM (2001) The prefrontal cortex - An update: Time is of the essence. *Neuron* 30:319–333. [https://doi.org/10.1016/S0896-6273\(01\)00285-9](https://doi.org/10.1016/S0896-6273(01)00285-9)

Gazzaley A, Rissman J, D'Esposito M (2004) Functional connectivity during working memory maintenance. *Cogn Affect Behav Neurosci* 4:580–599. <https://doi.org/10.3758/CABN.4.4.580>

Glasser MF, Coalson TS, Robinson EC, et al (2016) A multi-modal parcellation of human cerebral cortex. *Nature* 536:171–178. <https://doi.org/10.1038/nature18933>

Gorgolewski KJ, Varoquaux G, Rivera G, et al (2015) NeuroVault.Org: A web-based repository for collecting and sharing unthresholded statistical maps of the human brain. *Front Neuroinform* 9:1–9. <https://doi.org/10.3389/fninf.2015.00008>

Grosbras MH, Laird AR, Paus T (2005) Cortical regions involved in eye movements, shifts of attention, and gaze perception. *Hum Brain Mapp* 25:140–154. <https://doi.org/10.1002/hbm.20145>

Guo F, Preston TJ, Das K, et al (2012) Feature-Independent Neural Coding of Target Detection during Search of Natural Scenes. *J Neurosci* 32:9499–9510. <https://doi.org/10.1523/JNEUROSCI.5876-11.2012>

Gurel SC, Castelo-Branco M, Sack AT, Duecker F (2018) Assessing the Functional Role of Frontal Eye Fields in Voluntary and Reflexive Saccades Using Continuous Theta Burst Stimulation. *Front Neurosci* 12:1–11. <https://doi.org/10.3389/fnins.2018.00944>

Hakvoort Schwerdtfeger RM, Alahyane N, Brien DC, et al (2013) Preparatory neural networks are impaired in adults with attention-deficit/hyperactivity disorder during the antisaccade task. *NeuroImage Clin* 2:63–78. <https://doi.org/10.1016/j.nicl.2012.10.006>

Han SW, Marois R (2013) Dissociation between process-based and data-based limitations for conscious perception in the human brain. *Neuroimage* 64:399–406. <https://doi.org/10.1016/j.neuroimage.2012.09.016>

Han SW, Marois R (2014) Functional fractionation of the stimulus-driven attention network. *J Neurosci* 34:6958–6969. <https://doi.org/10.1523/JNEUROSCI.4975-13.2014>

Han SW, Shin H, Jeong D, et al (2018) Neural substrates of purely endogenous, self-regulatory control of attention. *Sci Rep* 8:1–10. <https://doi.org/10.1038/s41598-018-19508-6>

Hanes DP, Patterson WF, Schall JD (1998) Role of frontal eye fields in countermanding saccades: Visual, movement, and fixation activity. *J Neurophysiol* 79:817–834. <https://doi.org/10.1152/jn.1998.79.2.817>

Harding IH, Harrison BJ, Breakspear M, et al (2016) Cortical Representations of Cognitive Control and Working Memory Are Dependent Yet Non-Interacting. *Cereb Cortex* 26:557–565. <https://doi.org/10.1093/cercor/bhu208>

- Heinen SJ, Rowland J, Lee B, Wade AR (2006) An Oculomotor Decision Process Revealed by Functional Magnetic Resonance Imaging. *26*:13515–13522. <https://doi.org/10.1523/JNEUROSCI.4243-06.2006>
- Henseler I, Krüger S, Dechent P, Gruber O (2011) A gateway system in rostral PFC? Evidence from biasing attention to perceptual information and internal representations. *Neuroimage* 56:1666–1676. <https://doi.org/10.1016/j.neuroimage.2011.02.056>
- Hinds OP, Rajendran N, Polimeni JR, et al (2008) Accurate prediction of V1 location from cortical folds in a surface coordinate system. *Neuroimage* 39:1585–1599. <https://doi.org/10.1016/j.neuroimage.2007.10.033>
- Hinds O, Polimeni JR, Rajendran N, et al (2009) Locating the functional and anatomical boundaries of human primary visual cortex. *Neuroimage* 46:915–922. <https://doi.org/10.1016/j.neuroimage.2009.03.036>
- Huang CC, Rolls ET, Feng J, Lin CP (2022) An extended Human Connectome Project multimodal parcellation atlas of the human cortex and subcortical areas. *Brain Struct Funct* 227:763–778. <https://doi.org/10.1007/s00429-021-02421-6>
- Hubl D, Nyffeler T, Wurtz P, Chaves S (2008) Time course of blood oxygenation level–dependent signal response after theta burst transcranial magnetic stimulation of the frontal eye field. *Neuroscience* 151:921–928. <https://doi.org/10.1016/j.neuroscience.2007.10.049>
- Hupé JM, Bordier C, Dojat M (2012) A BOLD signature of eyeblinks in the visual cortex. *Neuroimage* 61:149–161. <https://doi.org/10.1016/j.neuroimage.2012.03.001>
- Hutton SB, Ettinger U (2006) The antisaccade task as a research tool in psychopathology: A critical review. *Psychophysiology* 43:302–313. <https://doi.org/10.1111/j.1469-8986.2006.00403.x>
- Jamadar SD, Fielding J, Egan GF (2013) Quantitative meta-analysis of fMRI and PET studies reveals consistent activation in fronto-striatal-parietal regions and cerebellum during antisaccades and prosaccades. *Front Psychol* 4:1–15. <https://doi.org/10.3389/fpsyg.2013.00749>
- Jamadar SD, Johnson BP, Clough M, et al (2015) Behavioral and neural plasticity of ocular motor control: Changes in performance and fMRI activity following antisaccade training. *Front Hum Neurosci* 9:1–13. <https://doi.org/10.3389/fnhum.2015.00653>
- Jarvstad A, Gilchrist ID (2019) Cognitive control of saccadic selection and inhibition from within the core cortical saccadic network. *J Neurosci* 39:2497–2508. <https://doi.org/10.1523/JNEUROSCI.1419-18.2018>
- Jerde TA, Merriam EP, Riggall AC, et al (2012) Prioritized maps of space in human frontoparietal cortex. *J Neurosci* 32:17382–17390. <https://doi.org/10.1523/JNEUROSCI.3810-12.2012>
- Ji JL, Spronk M, Kulkarni K, et al (2019) Mapping the human brain’s cortical-subcortical functional network organization. *Neuroimage* 185:35–57. <https://doi.org/10.1016/j.neuroimage.2018.10.006>
- Juch H, Zimine I, Seghier ML, et al (2005) Anatomical variability of the lateral frontal lobe surface: Implication for intersubject variability in language neuroimaging. *Neuroimage* 24:504–514. <https://doi.org/10.1016/j.neuroimage.2004.08.037>
- Kanwisher N (2010) Functional specificity in the human brain: A window into the functional architecture of the mind. *Proc Natl Acad Sci U S A* 107:11163–11170. <https://doi.org/10.1073/pnas.1005062107>
- Kastner S, DeSimone K, Konen CS, et al (2007) Topographic maps in human frontal cortex revealed in memory-guided saccade and spatial working-memory tasks. *J Neurophysiol* 97:3494–3507. <https://doi.org/10.1152/jn.00010.2007>
- Kato M, Miyauchi S (2003) Human precentral cortical activation patterns during saccade tasks: An fMRI comparison with activation during intentional eyeblink tasks. *Neuroimage* 19:1260–1272. [https://doi.org/10.1016/S1053-8119\(03\)00223-4](https://doi.org/10.1016/S1053-8119(03)00223-4)

Kim C, Johnson NF, Gold BT (2012) Common and distinct neural mechanisms of attentional switching and response conflict. *Brain Res* 1469:92–102. <https://doi.org/10.1016/j.brainres.2012.06.013>

Koyama M, Hasegawa I, Osada T, et al (2004) Functional magnetic resonance imaging of macaque monkeys performing visually guided saccade tasks: Comparison of cortical eye fields with humans. *Neuron* 41:795–807. [https://doi.org/10.1016/S0896-6273\(04\)00047-9](https://doi.org/10.1016/S0896-6273(04)00047-9)

Kurata J, Thulborn KR, Firestone LL (2005) The cross-modal interaction between pain-related and saccade-related cerebral activation: A preliminary study by event-related functional magnetic resonance imaging. *Anesth Analg* 101:449–456. <https://doi.org/10.1213/01.ANE.0000158468.84424.5D>

Lancaster JL, Woldorff MG, Parsons LM, et al (2000) Automated Talairach Atlas labels for functional brain mapping. *Hum Brain Mapp* 10:120–131. [https://doi.org/10.1002/1097-0193\(200007\)10:3<120::AID-HBM30>3.0.CO;2-8](https://doi.org/10.1002/1097-0193(200007)10:3<120::AID-HBM30>3.0.CO;2-8)

Lancaster JL, Laird AR, Eickhoff SB, et al (2012) Automated regional behavioral analysis for human brain images. *Front Neuroinform* 6:1–12. <https://doi.org/10.3389/fninf.2012.00023>

Langner R, Camilleri JA (2021) Meta-Analytic Connectivity Modelling (MACM): A Tool for Assessing Region-Specific Functional Connectivity Patterns in Task-Constrained States. In: Diwadkar, V.A., B. Eickhoff, S. (eds) *Brain Network Dysfunction in Neuropsychiatric Illness*. Springer, Cham. [https://doi.org/10.1007/978-3-030-59797-9\\_5](https://doi.org/10.1007/978-3-030-59797-9_5)

Langner R, Rottschy C, Laird AR, et al (2014) Meta-analytic connectivity modeling revisited: Controlling for activation base rates. *Neuroimage* 99:559–570. <https://doi.org/10.1016/j.neuroimage.2014.06.007>

Levy I, Schluppeck D, Heeger DJ, Glimcher PW (2007) Specificity of human cortical areas for reaches and saccades. *J Neurosci* 27:4687–4696. <https://doi.org/10.1523/JNEUROSCI.0459-07.2007>

Lin H, Li WP, Carlson S (2019) A privileged working memory state and potential top-down modulation for faces, not scenes. *Front Hum Neurosci* 13:1–10. <https://doi.org/10.3389/fnhum.2019.00002>

Liu T (2016) Neural representation of object-specific attentional priority. *Neuroimage* 129:15–24. <https://doi.org/10.1016/j.neuroimage.2016.01.034>

Liu T, Hospadaruk L, Zhu DC, Gardner JL (2011) Feature-specific attentional priority signals in human cortex. *J Neurosci* 31:4484–4495. <https://doi.org/10.1523/JNEUROSCI.5745-10.2011>

Lowe KA, Schall JD (2018) Functional categories of visuomotor neurons in macaque frontal eye field. *eNeuro* 5:1–21. <https://doi.org/10.1523/ENEURO.0131-18.2018>

Luna B, Thulborn KR, Strojwas MH, et al (1998) Dorsal cortical regions subserving visually guided saccades in humans: An fMRI study. *Cereb Cortex* 8:40–47. <https://doi.org/10.1093/cercor/8.1.40>

Mackey WE, Winawer J, Curtis CE (2017) Visual field map clusters in human frontoparietal cortex. *Elife* 6:1–23. <https://doi.org/10.7554/eLife.22974>

Markiewicz CJ, Gorgolewski KJ, Feingold F, et al (2021) The openneuro resource for sharing of neuroscience data. *Elife* 10:1–17. <https://doi.org/10.7554/eLife.71774>

Mars RB, Jbabdi S, Rushworth MFS (2021) A Common Space Approach to Comparative Neuroscience. *Annu Rev Neurosci* 44:69–86. <https://doi.org/10.1146/annurev-neuro-100220-025942>

McDowell JE, Dyckman KA, Austin BP, Clementz BA (2008) Neurophysiology and neuroanatomy of reflexive and volitional saccades: Evidence from studies of humans. *Brain Cogn* 68:255–270. <https://doi.org/10.1016/j.bandc.2008.08.016>

Melcher T, Gruber O (2006) Oddball and incongruity effects during Stroop task performance: A comparative fMRI study on selective attention. *Brain Res* 1121:136–149. <https://doi.org/10.1016/j.brainres.2006.08.120>

- Mesulam MM (1998) From sensation to cognition. *Brain* 121:1013–1052. <https://doi.org/10.1093/brain/121.6.1013>
- Miller EK, Cohen JD (2001) An integrative theory of prefrontal cortex function. *Annu Rev Neurosci* 24:167–202. <https://doi.org/10.1146/annurev.neuro.24.1.167>
- Miller JA, Voorhies WI, Lurie DJ, et al (2021) Overlooked tertiary sulci serve as a meso-scale link between microstructural and functional properties of human lateral prefrontal cortex. *J Neurosci* 41:2229–2244. <https://doi.org/10.1523/jneurosci.2362-20.2021>
- Mills K (2016) HCP-MMP1.0 projected on fsaverage. <https://doi.org/10.6084/m9.figshare.3498446.v2>
- Moore T, Fallah M (2001) Control of eye movements and spatial attention. *Proc Natl Acad Sci U S A* 98:1273–1276. <https://doi.org/10.1073/pnas.98.3.1273>
- Muhle-Karbe PS, Derrfuss J, Lynn MT, et al (2016) Co-Activation-Based Parcellation of the Lateral Prefrontal Cortex Delineates the Inferior Frontal Junction Area. *Cereb Cortex* 26:2225–2241. <https://doi.org/10.1093/cercor/bhv073>
- Müller VI, Cieslik EC, Laird AR, et al (2018) Ten simple rules for neuroimaging meta-analysis. *Neurosci Biobehav Rev* 84:151–161. <https://doi.org/10.1016/j.neubiorev.2017.11.012>
- Nee DE, Brown JW, Askren MK, et al (2013) A meta-Analysis of executive components of working memory. *Cereb Cortex* 23:264–282. <https://doi.org/10.1093/cercor/bhs007>
- Neggers SFW, Huijbers W, Vrijlandt CM, et al (2007) TMS Pulses on the Frontal Eye Fields Break Coupling Between Visuospatial Attention and Eye Movements. *J Neurophysiol* 98:2765–2778. <https://doi.org/10.1152/jn.00357.2007>
- Neggers SFW, Zandbelt BB, Schall MS, Schall JD (2015) Comparative diffusion tractography of corticostriatal motor pathways reveals differences between humans and macaques. *J Neurophysiol* 113:2164–2172. <https://doi.org/10.1152/jn.00569.2014>
- Neubert FX, Mars RB, Thomas AG, et al (2014) Comparison of Human Ventral Frontal Cortex Areas for Cognitive Control and Language with Areas in Monkey Frontal Cortex. *Neuron* 81:700–713. <https://doi.org/10.1016/j.neuron.2013.11.012>
- Ngo GH, Eickhoff SB, Nguyen M, et al (2019) Beyond consensus: Embracing heterogeneity in curated neuroimaging meta-analysis. *Neuroimage* 200:142–158. <https://doi.org/10.1016/j.neuroimage.2019.06.037>
- Numssen O, Bzdok D, Hartwigsen G (2021) Functional specialization within the inferior parietal lobes across cognitive domains. *Elife* 10:1–25. <https://doi.org/10.7554/eLife.63591>
- O’Craven KM, Downing PE, Kanwisher N (1999) fMRI evidence for objects as the units of attentional selection. *Nature* 401:584–587. <https://doi.org/10.1038/44134>
- O’Reilly RC (2010) The What and how of prefrontal cortical organization. *Trends Neurosci* 33:355–361. <https://doi.org/10.1016/j.tins.2010.05.002>
- Ono M, Kubik S, Abernathy CD (1990) *Atlas of the cerebral sulci*. Thieme Medical Publishers.
- Osher DE, Saxe RR, Koldewyn K, et al (2016) Structural Connectivity Fingerprints Predict Cortical Selectivity for Multiple Visual Categories across Cortex. *Cereb Cortex* 26:1668–1683. <https://doi.org/10.1093/cercor/bhu303>
- Owen AM, Stern CE, Look RB, et al (1998) Functional organization of spatial and nonspatial working memory processing within the human lateral frontal cortex. *Proc Natl Acad Sci U S A* 95:7721–7726. <https://doi.org/10.1073/pnas.95.13.7721>

- Page MJ, McKenzie JE, Bossuyt PM, et al (2021) The PRISMA 2020 statement: An updated guideline for reporting systematic reviews. *BMJ* 372:1–9. <https://doi.org/10.1136/bmj.n71>
- Parlatini V, Radua J, Acqua FD, et al (2017) Functional segregation and integration within fronto-parietal networks. *Neuroimage* 146:367–375. <https://doi.org/10.1016/j.neuroimage.2016.08.031>
- Passingham RE, Stephan KE, Kötter R (2002) The anatomical basis of functional localization in the cortex. *Nat Rev Neurosci* 3:606–616. <https://doi.org/10.1038/nrn893>
- Paus T (1996) Location and function of the human frontal eye- field : A selective review. *Neuropsychologia* 34:475–483. [https://doi.org/10.1016/0028-3932\(95\)00134-4](https://doi.org/10.1016/0028-3932(95)00134-4)
- Peelen M V., Downing PE (2005) Selectivity for the human body in the fusiform gyrus. *J Neurophysiol* 93:603–608. <https://doi.org/10.1152/jn.00513.2004>
- Petrides M (2018) *Atlas of the morphology of the human cerebral cortex on the average MNI brain*. Academic Press.
- Petit L, Pouget P (2019) The comparative anatomy of frontal eye fields in primates. *Cortex* 118:51–64. <https://doi.org/10.1016/j.cortex.2019.02.023>
- Pierce JE, Saj A, Vuilleumier P (2019) Differential parietal activations for spatial remapping and saccadic control in a visual memory task. *Neuropsychologia* 131:129–138. <https://doi.org/10.1016/j.neuropsychologia.2019.05.010>
- Pierrot-Deseilligny C, Ploner CJ, Müri RM, et al (2002) Effects of cortical lesions on saccadic eye movements in humans. *Ann N Y Acad Sci* 956:216–229. <https://doi.org/10.1111/j.1749-6632.2002.tb02821.x>
- Poldrack RA (2011) Inferring mental states from neuroimaging data: From reverse inference to large-scale decoding. *Neuron* 72:692–697. <https://doi.org/10.1016/j.neuron.2011.11.001>
- Posner MI, Snyder CR, Davidson BJ (1980) Attention and the detection of signals. *J Exp Psychol Gen* 109:160–174. <https://doi.org/10.1037/0096-3445.109.2.160>
- Reid AT, Bzdok D, Genon S, et al (2016) ANIMA: A data-sharing initiative for neuroimaging meta-analyses. *Neuroimage* 124:1245–1253. <https://doi.org/10.1016/j.neuroimage.2015.07.060>
- Robinson EC, Garcia K, Glasser MF, et al (2018) Multimodal surface matching with higher-order smoothness constraints. *Neuroimage* 167:453–465. <https://doi.org/10.1016/j.neuroimage.2017.10.037>
- Robinson JL, Laird AR, Glahn DC, et al (2010) Metaanalytic connectivity modeling: Delineating the functional connectivity of the human amygdala. *Hum Brain Mapp* 31:173–184. <https://doi.org/10.1002/hbm.20854>
- Roth JK, Serences JT, Courtney SM (2006) Neural system for controlling the contents of object working memory in humans. *Cereb Cortex* 16:1595–1603. <https://doi.org/10.1093/cercor/bhj096>
- Rottschy C, Langner R, Dogan I, et al (2012) Modelling neural correlates of working memory: A coordinate-based meta-analysis. *Neuroimage* 60:830–846. <https://doi.org/10.1016/j.neuroimage.2011.11.050>
- Ruland SH, Palomero-Gallagher N, Hoffstaedter F, et al (2022) The inferior frontal sulcus: Cortical segregation, molecular architecture and function. *Cortex* 153:235–256. <https://doi.org/10.1016/j.cortex.2022.03.019>
- Saslow MG (1967) Effects of components of displacement-step stimuli upon latency for saccadic eye movement. *J Opt Soc Am* 57:1024–1029. <https://doi.org/10.1364/JOSA.57.001024>
- Saygin ZM, Osher DE, Koldewyn K, et al (2012) Anatomical connectivity patterns predict face selectivity in the fusiform gyrus. *Nat Neurosci* 15:321–327. <https://doi.org/10.1038/nn.3001>



- Sallet J, Mars RB, Noonan MP, et al (2013) The Organization of Dorsal Frontal Cortex in Humans and Macaques. *J Neurosci* 33:12255–12274. <https://doi.org/10.1523/JNEUROSCI.5108-12.2013>
- Schall JD, Hanes DP (1998) Neural mechanisms of selection and control of visually guided eye movements. *Neural Networks* 11:1241–1251. [https://doi.org/10.1016/S0893-6080\(98\)00059-8](https://doi.org/10.1016/S0893-6080(98)00059-8)
- Schall JD (2015) Visuomotor Functions in the Frontal Lobe. *Annu Rev Vis Sci* 1:469–498. <https://doi.org/10.1146/annurev-vision-082114-035317>
- Schall JD, Zinke W, Cosman JD, et al (2020) On the Evolution of the Frontal Eye Field: Comparisons of Monkeys, Apes, and Humans. *Evol Neurosci* 861–890. <https://doi.org/10.1016/b978-0-12-820584-6.00036-2>
- Scheperjans F, Hermann K, Eickhoff SB, et al (2008) Observer-independent cytoarchitectonic mapping of the human superior parietal cortex. *Cereb Cortex* 18:846–867. <https://doi.org/10.1093/cercor/bhm116>
- Scheperjans F, Eickhoff SB, Hömke L, et al (2008) Probabilistic maps, morphometry, and variability of cytoarchitectonic areas in the human superior parietal cortex. *Cereb Cortex* 18:2141–2157. <https://doi.org/10.1093/cercor/bhm241>
- Schon K, Tinaz S, Somers DC, Stern CE (2008) Delayed match to object or place: An event-related fMRI study of short-term stimulus maintenance and the role of stimulus pre-exposure. *Neuroimage* 39:857–872. <https://doi.org/10.1016/j.neuroimage.2007.09.023>
- Schmitt O, Modersitzki J, Heldmann S et al. (2005) Three-dimensional cytoarchitectonic analysis of the posterior bank of the human precentral sulcus. *Anat Embryol* 210: 387–400. <https://doi.org/10.1007/s00429-005-0030-8>
- Sereno MI, Dale AM, Reppas JB, Kwong KK, Belliveau JW, Brady TJ, Rosen BR, Tootell RBH (1995) Borders of multiple visual areas in humans revealed by functional magnetic resonance imaging. *Science* 268:889–893. <https://doi.org/10.1126/science.7754376>
- Sreenivasan KK, Gratton C, Vytlačil J, D’Esposito M (2014) Evidence for working memory storage operations in perceptual cortex. *Cogn Affect Behav Neurosci* 14:117–128. <https://doi.org/10.3758/s13415-013-0246-7>
- Stelzel C, Basten U, Fiebach CJ (2011) Functional connectivity separates switching operations in the posterior lateral frontal cortex. *J Cogn Neurosci* 23:3529–3539. [https://doi.org/10.1162/jocn\\_a\\_00062](https://doi.org/10.1162/jocn_a_00062)
- Stiers P, Goulas A (2018) Functional connectivity of task context representations in prefrontal nodes of the multiple demand network. *Brain Struct Funct* 223:2455–2473. <https://doi.org/10.1007/s00429-018-1638-9>
- Sundermann B, Pfeleiderer B (2012) Functional connectivity profile of the human inferior frontal junction: Involvement in a cognitive control network. *BMC Neurosci* 13:1–13. <https://doi.org/10.1186/1471-2202-13-119>
- Tamber-Rosenau BJ, Asplund CL, Marois R (2018) Functional dissociation of the inferior frontal junction from the dorsal attention network in top-down attentional control. *J Neurophysiol* 120:2498–2512. <https://doi.org/10.1152/jn.00506>
- Tark KJ, Curtis CE (2009) Persistent neural activity in the human frontal cortex when maintaining space that is off the map. *Nat Neurosci* 12:1463–1468. <https://doi.org/10.1038/nn.2406>
- Tehovnik EJ, Sommer MA, Chou IH, et al (2000) Eye fields in the frontal lobes of primates. *Brain Res Rev* 32:413–448. [https://doi.org/10.1016/S0165-0173\(99\)00092-2](https://doi.org/10.1016/S0165-0173(99)00092-2)
- Tibber M, Saygin AP, Grant S, et al (2010) The neural correlates of visuospatial perceptual and oculomotor extrapolation. *PLoS One* 5:1–12. <https://doi.org/10.1371/journal.pone.0009664>
- Todd JJ, Han SW, Harrison S, Marois R (2011) The neural correlates of visual working memory encoding: A time-resolved fMRI study. *Neuropsychologia* 49:1527–1536. <https://doi.org/10.1016/j.neuropsychologia.2011.01.040>

- Toro R, Perron M, Pike B, et al (2008) Brain size and folding of the human cerebral cortex. *Cereb Cortex* 18:2352–2357. <https://doi.org/10.1093/cercor/bhm261>
- Tu PC, Yang TH, Kuo WJ, et al (2006) Neural correlates of antisaccade deficits in schizophrenia, an fMRI study. *J Psychiatr Res* 40:606–612. <https://doi.org/10.1016/j.jpsychires.2006.05.012>
- Van Essen DC (2007) Cerebral cortical folding patterns in primates: Why they vary and what they signify. *Evol Nerv Syst* 4:267–276. <https://doi.org/10.1016/B0-12-370878-8/00344-X>
- Van Essen DC, Smith SM, Barch DM, et al (2013) The WU-Minn Human Connectome Project: An overview. *Neuroimage* 80:62–79. <https://doi.org/10.1016/j.neuroimage.2013.05.041>
- Van Essen DC, Smith J, Glasser MF, et al (2017) The Brain Analysis Library of Spatial maps and Atlases (BALSAL) database. *Neuroimage* 144:270–274. <https://doi.org/https://doi.org/10.1016/j.neuroimage.2016.04.002>
- Verbruggen F, Aron AR, Stevens MA, Chambers CD (2010) Theta burst stimulation dissociates attention and action updating in human inferior frontal cortex. *Proc Natl Acad Sci U S A* 107:13966–13971. <https://doi.org/10.1073/pnas.1001957107>
- Vernet M, Quentin R, Chanes L, et al (2014) Frontal eye field, where art thou? Anatomy, function, and non-invasive manipulation of frontal regions involved in eye movements and associated cognitive operations. *Front Integr Neurosci*. <https://doi.org/10.3389/fnint.2014.00066>
- Wang L, Mruzec REB, Arcaro MJ, Kastner S (2015) Probabilistic maps of visual topography in human cortex. *Cereb Cortex* 25:3911–3931. <https://doi.org/10.1093/cercor/bhu277>
- Welker W (1990) Why does cerebral cortex fissure and fold? In *Cerebral cortex* (pp. 3-136). Springer, Boston, MA.
- Wills KM, Liu J, Hakun J, et al (2017) Neural Mechanisms for the Benefits of Stimulus-Driven Attention. *Cereb Cortex* 27:5294–5302. <https://doi.org/10.1093/cercor/bhw308>
- Yeo BTT, Krienen FM, Sepulcre J, et al (2011) The organization of the human cerebral cortex estimated by intrinsic functional connectivity. *J Neurophysiol* 106:1125–1165. <https://doi.org/10.1152/jn.00338.2011>
- Yin S, Deák G, Chen A (2018) Coactivation of cognitive control networks during task switching. *Neuropsychology* 32:31–39. <https://doi.org/10.1037/neu0000406>
- Young MP, Hilgetag CC, Scannell JW (2000) On imputing function to structure from the behavioural effects of brain lesions. *Philos Trans R Soc B Biol Sci* 355:147–161. <https://doi.org/10.1098/rstb.2000.0555>
- Zanto TP, Rubens MT, Bollinger J, Gazzaley A (2010) Top-down modulation of visual feature processing: The role of the inferior frontal junction. *Neuroimage* 53:736–745. <https://doi.org/10.1016/j.neuroimage.2010.06.012>
- Zanto TP, Rubens MT, Thangavel A, Gazzaley A (2011) Causal role of the prefrontal cortex in top-down modulation of visual processing and working memory. *Nat Neurosci* 14:656–663. <https://doi.org/10.1038/nn.2773>
- Zhang X, Mlynaryk N, Ahmed S, et al (2018) The role of inferior frontal junction in controlling the spatially global effect of feature-based attention in human visual areas. *PLoS Biol* 16:1–28. <https://doi.org/10.1371/journal.pbio.2005399>
- Zhao Y, Kuai S, Zanto TP, Ku Y (2020) Neural Correlates Underlying the Precision of Visual Working Memory. *Neuroscience* 425:301–311. <https://doi.org/10.1016/j.neuroscience.2019.11.037>
- Zilles K, Palomero-Gallagher N, Amunts K (2013) Development of cortical folding during evolution and ontogeny. *Trends Neurosci* 36:275–284. <https://doi.org/10.1016/j.tins.2013.01.006>

## Supplementary Figures and Tables

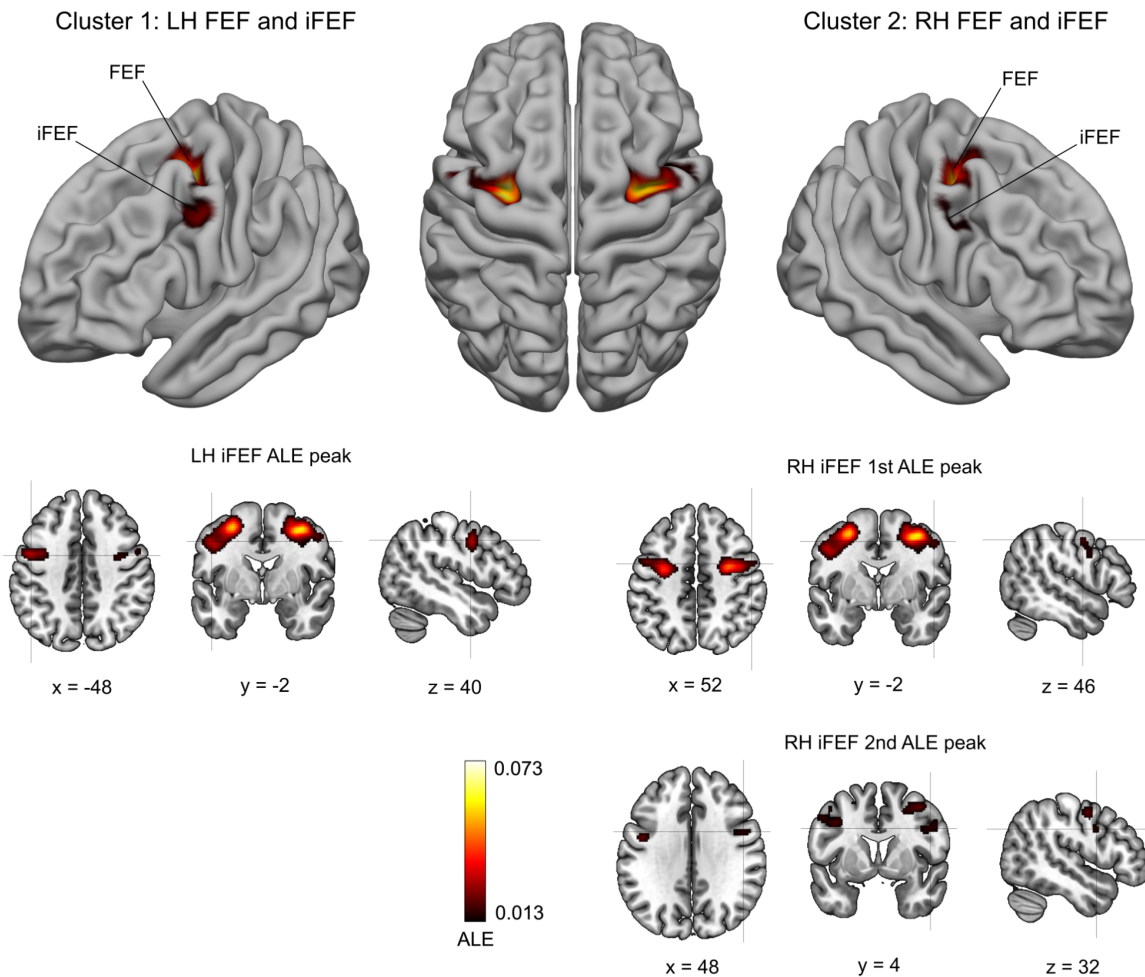


**Figure S1.** Results of the first FEF sample control analysis. Applying cluster-level FWE in the ALE analysis allowed us to uncover bilateral activations ventral to the main FEF peaks. These activations were extending from the sPCS to the posterior bank of the iPCS, and were primarily localized in the precentral gyrus. These results reveal the presence of consistent iFEF activations in the FEF localizer sample and three iFEF peaks (shown at the bottom of the figure).

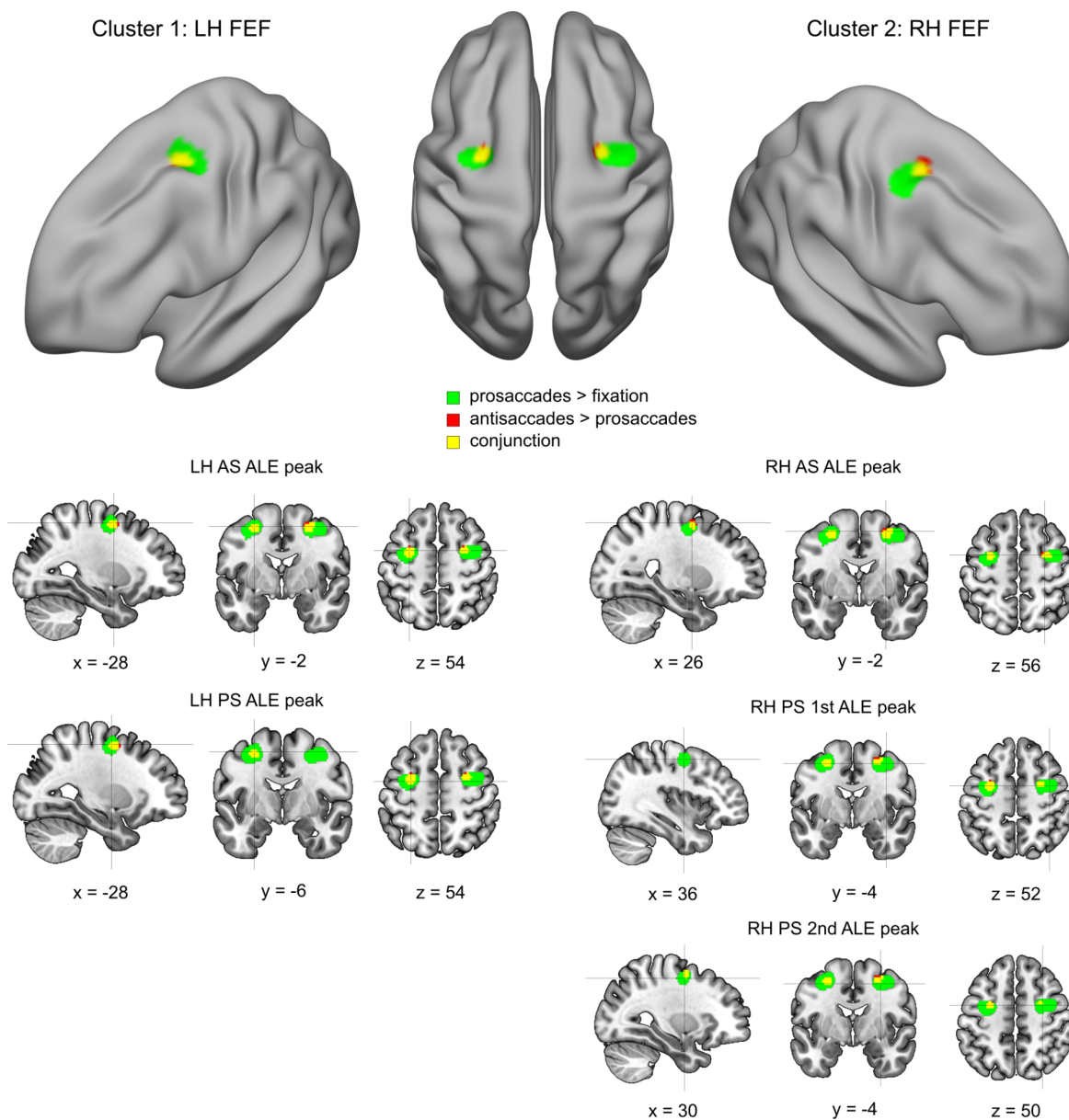


**Figure S2.** Second FEF control analysis comparing the topography of antisaccade > prosaccade (AS) with prosaccade > fixation (PS) contrasts. The clusters overlap in the bilateral posterior aspect of the SFS. The disjunction of these clusters showed that the AS clusters were generally more medial and localized anterior to the PS clusters. These results are consistent with those reported in Cieslik et al. (2016).

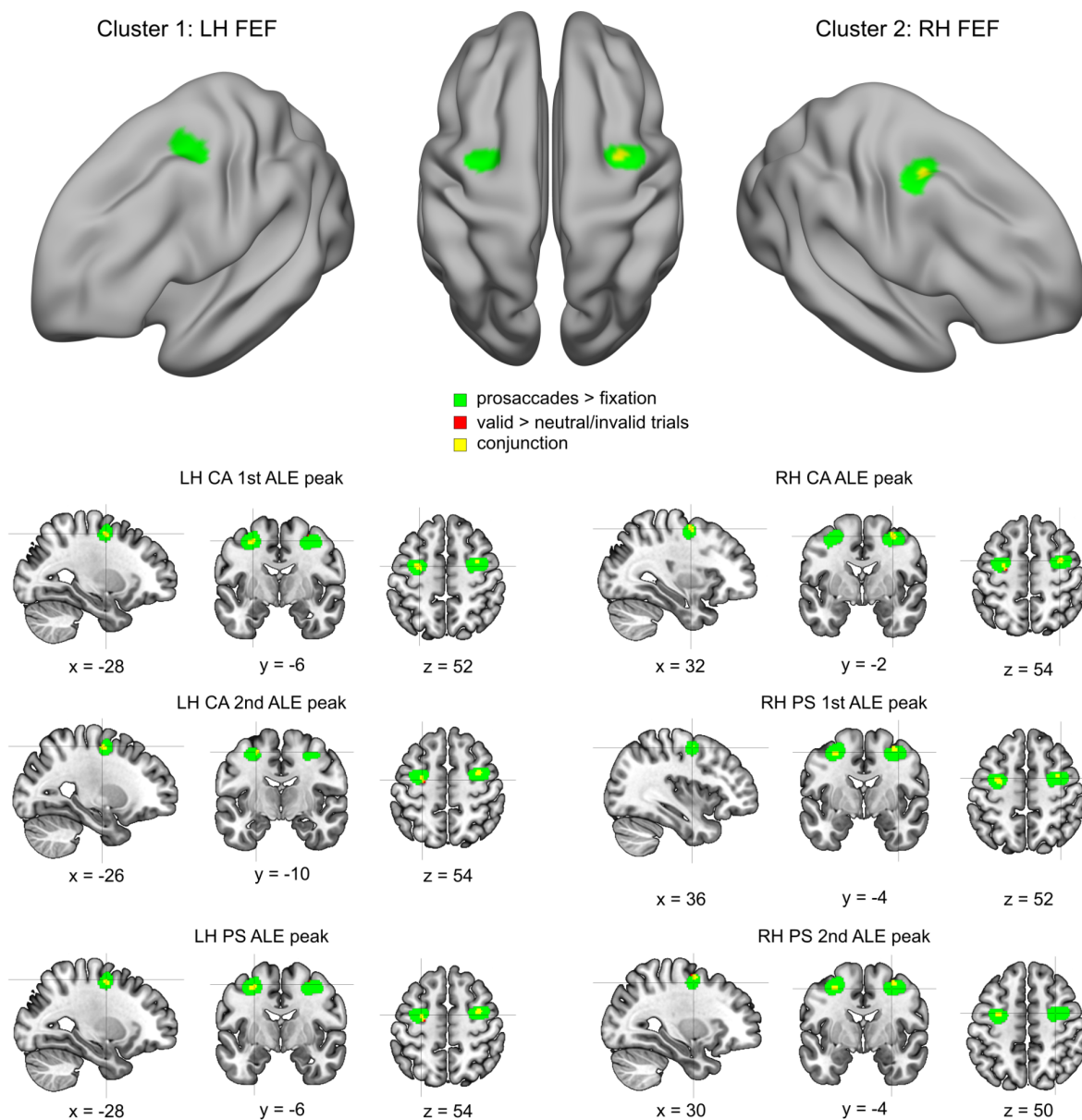


**Figure S3.** Third FEF control analysis comparing the topography of prosaccades > fixation (PS) vs valid > neutral/invalid trials in covert spatial attention (CA) task contrasts.



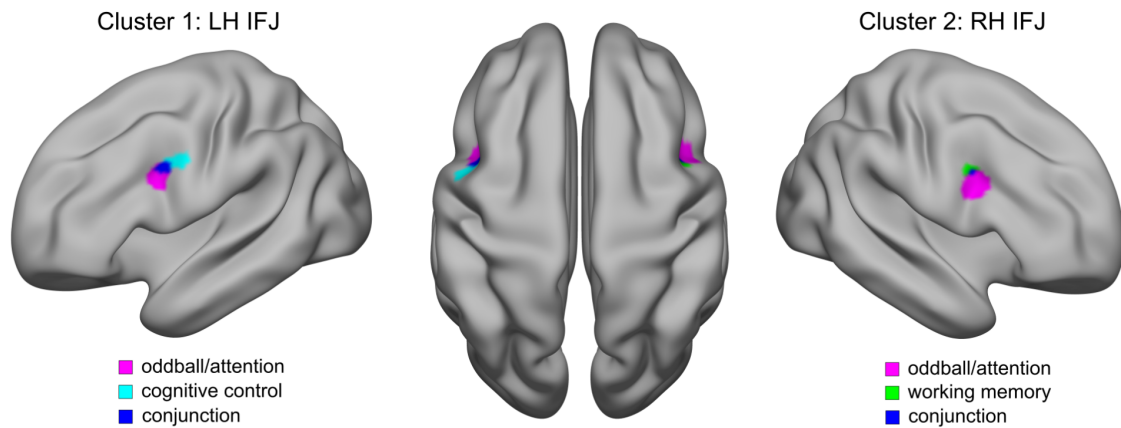


**Figure S4.** Results of the IFJ sample control analysis. The IFJ sample was split in three groups of experiments based on the paradigm employed (oddball/cueing vs n-back vs task-switching/Stroop) to explore potential spatial dissociations between them. In line with this possibility, we found a lateralized cluster involved in cognitive control (i.e., task-switching/Stroop paradigms) in the left hemisphere, and a cluster involved in working memory (mainly n-back contrasts) in the right hemisphere. While these clusters overlapped with a bilateral cluster associated with oddball/attention contrasts at the iPCS and IFS junction, near the putative IFJ, the latter were generally anterior and ventral relative to their location in both hemispheres (see the regions shown in purple).

**Table S1.** List of the studies included in the proscenades > fixation analysis

Study	N	Age	Paradigm	Contrast	Scanner	Design	Eye tracker	Results reported for	N° of foci	Multiple FEF foci	Software	Space
<a href="#">Alkon et al. (2011)</a>	8	26 ± 4	Functional localizer	Pro-scenades > Fixation	3T	Blocked	Y	Whole-brain	19	N	AFNI	Talairach
<a href="#">Amiez and Dericqes (2018)</a>	13	22.6 ± 2.8	Functional localizer	Pro-scenades > Fixation	3T	Blocked	N	FEF foci	2	N	SPM12b	MNI
<a href="#">Amiez et al. (2013)</a>	11	26.9; 22-33	Functional localizer	Pro-scenades > Fixation	3T	Blocked	N	Whole-brain	24	Y	SPM8	MNI
<a href="#">Bair et al. (2016)</a>	14	22-56	Functional localizer	Pro-scenades > Fixation	3T	Blocked	N	Whole-brain	12	N	Brain Voyager QX 1.10	Talairach
<a href="#">Berman et al. (1999)</a>	11	25.6 ± 7.1; 18-43	Functional localizer	Pro-scenades > Fixation	3T	Blocked	N	ROIs	14	Y	AFNI	Talairach
<a href="#">Braga et al. (2016)</a>	20	26.2; 21-36	Functional localizer	Pro-scenades > Fixation	3T	Blocked	Y	Whole-brain	7	N	FSL	MNI
<a href="#">Brown et al. (2006)</a>	10	26; 22-33	Functional localizer	Pro-scenades > Fixation	4T	<i>Event-related</i>	Y	Whole-brain	17	N	Brain Voyager 2000	Talairach
<a href="#">Connolly et al. (2000)</a>	7	24.8 ± 3.2	Functional localizer	Pro-scenades > Fixation	4T	Blocked	N	Whole-brain	7	Y	Stimulate	Talairach
<a href="#">Connolly et al. (2002)</a>	8	NA	Functional localizer	Pro-scenades > Fixation	4T	Blocked	N	ROIs	4	N	Stimulate	Talairach
<a href="#">Connolly et al. (2005)</a>	5	NA	Functional localizer	Pro-scenades > Fixation	4T	Blocked	Y	ROIs	5	N	Stimulate / Brain Voyager 4.9	Talairach
<a href="#">Connolly et al. (2007)</a>	8	NA	Functional localizer	Pro-scenades > Fixation	4T	Blocked	N	ROIs	2	Y	Stimulate / Brain Voyager 4.9 / QX	Talairach
<a href="#">Christophel et al. (2018)</a>	22	24.4 ± 0.83	Functional localizer	Pro-scenades > Fixation	3T	<i>Event-related</i>	N	FEF foci	2	N	SPM8	MNI
<a href="#">Dücker et al. (2013)</a>	20	19-28	Functional localizer	Pro-scenades > Fixation	3T	Blocked	N	FEF foci	2	N	Brain Voyager QX 2.3	Talairach
<a href="#">Emmerson et al. (2014)</a>	24	26.7 ± 4.9	Functional localizer	Pro-scenades > Fixation	3T	Blocked	Y	Whole-brain	8	N	SPM8	MNI
<a href="#">Gao et al. (2012)</a>	12	19-31	Functional localizer	Pro-scenades > Fixation	3T	Blocked	Y	ROIs	6	N	SPM8	Talairach
<a href="#">Garel et al. (2018)</a>	16	23.2	Functional localizer	Pro-scenades > Fixation	3T	Blocked	Y	FEF foci	2	N	Brain Voyager QX	Talairach
<a href="#">Heinen et al. (2006)</a>	5	20-37	Functional localizer	Pro-scenades > Fixation	3T	Blocked	Y	ROIs	4	N	VISTA/SOFT	Talairach
<a href="#">Hübli et al. (2008)</a>	7	31 ± 9	Functional localizer	Pro-scenades > Fixation	3T	Blocked	Y	Whole-brain	9	N	Brain Voyager QX	Talairach
<a href="#">Jänndar et al. (2015)</a>	23	25.8; 18-43	Functional localizer	Pro-scenades > Fixation	3T	<i>Event-related</i>	Y	Whole-brain	47	N	SPM8	MNI
<a href="#">Jänndar &amp; Gilchrist (2019)</a>	23	NA	Functional localizer	Pro-scenades > Fixation	3T	Blocked	Y	Whole-brain	4	N	FSL v.5.06-1	MNI
<a href="#">Kastner et al. (2007)</a>	4	20-36	Functional localizer	Pro-scenades > Fixation	3T	Blocked	Y	ROIs	5	N	AFNI	Talairach
<a href="#">Kurita et al. (2005)</a>	6	29-38	Functional localizer	Pro-scenades > Fixation	3T	Blocked	N	Whole-brain	14	N	Advanced Visual Systems & AFNI	Talairach
<a href="#">Levy et al. (2007)</a>	4	24-43	Functional localizer	Pro-scenades > Fixation	3T	Blocked	N	ROIs	5	N	Brain Voyager QX	Talairach
<a href="#">Marrero et al. (2003)</a>	12	20-42	Functional localizer	Pro-scenades > Fixation	3T	Blocked	N	FEF foci	1	N	SPM99	MNI
<a href="#">Pierce et al. (2019)</a>	30	25.7 ± 4.1	Functional localizer	Pro-scenades > Fixation	3T	Blocked	Y	Whole-brain	9	Y	SPM12	MNI
<a href="#">Schon et al. (2008)</a>	17	21.29 ± 3.72	Functional localizer	Pro-scenades > Fixation	3T	Blocked	N	Whole-brain	19	N	SPM2	MNI
<a href="#">Tambar-Kosenman et al. (2018)</a>	8	28.5 ± 3.3	Functional localizer	Pro-scenades > Fixation	3T	Blocked	Y	ROIs	6	N	Brain Voyager QX v.1.10.2-2.8	Talairach
<a href="#">Tark &amp; Curtis (2009)</a>	5	22-39	Functional localizer	Pro-scenades > Fixation	3T	Blocked	Y	FEF foci	2	N	Caret	MNI
<a href="#">Tibbet et al. (2010)</a>	16	21-40	Functional localizer	Pro-scenades > Fixation	3T	Blocked	Y	ROIs	9	N	SPM5	Talairach

**Table S2.** List of the studies included in the antisaccades > prosaccades contrast

Study	N	Age	Paradigm	Contrast	Scanner	Design	Eye tracker	Results reported for	N° of foci	Software	Space
<a href="#">Brown et al. (2006)</a>	10	26; 22-33	Antisaccade paradigm	Antisaccades > Prosaccades trials	4T	Event-related	Y	Whole-brain	15	Brain Voyager 2000	Talairach
<a href="#">Brown et al. (2007)</a>	11	25; 20-28	Antisaccade paradigm	Antisaccades > Prosaccades trials	4T	Event-related	Y	Whole-brain	14	Brain Voyager 2000	Talairach
<a href="#">Brown et al. (2007)</a>	11	25; 20-28	Antisaccade paradigm	Antisaccades > Prosaccades trials	4T	Event-related	Y	Whole-brain	11	Brain Voyager 2000	Talairach
<a href="#">Cameron et al. (2009)</a>	11	22-30	Antisaccade paradigm	Antisaccades > Prosaccades trials	3T	Event-related	Y	FEF foci	2	Brain Voyager 1.9	Talairach
<a href="#">Ford et al. (2005)</a>	10	28	Antisaccade paradigm	Antisaccades > Prosaccades trials	4T	Event-related	Y	Whole-brain	8	Brain Voyager 2000 v. 4.8	Talairach
<a href="#">Manoach et al. (2007)</a>	21	34.2 ± 12.6	Antisaccade paradigm	Antisaccades > Prosaccades trials	3T	Event-related	Y	Whole-brain	7	FreeSurfer	Talairach
<a href="#">Neggers et al. (2012)</a>	13	20-35	Antisaccade paradigm	Antisaccades > Prosaccades trials	3T	Event-related	N	ROIs	13	SPM5	MNI
<a href="#">Peirce &amp; McDowell (2016)</a>	35	19 ± 3.5	Antisaccade paradigm	Antisaccades > Prosaccades trials	3T	Event-related	Y	Whole-brain	5	AFNI	Talairach
<a href="#">Peirce &amp; McDowell (2017)</a>	35	19 ± 3.5	Antisaccade paradigm	Antisaccades > Prosaccades blocks	3T	Blocked	Y	Whole-brain	2	AFNI	Talairach
<a href="#">Salvia et al. (2020)</a>	14	27.1 ± 2.7	Antisaccade paradigm	Antisaccades > Prosaccades trials	3T	Event-related	Y	Whole-brain	12	SPM12	MNI

**Table S3.** List of the studies included in the endogenous covert spatial attention analysis

Study	N	Age	Paradigm	Contrast	Scanner	Design	Eye tracker	Results reported for	N° of foci	Multiple FEF foci	Software	Space
<a href="#">Chica et al. (2013)</a>	18	25 ± 4	Spatial cueing	Cue > Jitter Fixation	3T	Event-related	N	Whole-brain	22	Y	SPM5	MNI
<a href="#">Fan et al. (2005)</a>	16	27.2 ± 5.7	Attentional network test	Spatial > Center cue	3T	Event-related	N	Whole-brain	8	N	SPM99	MNI
<a href="#">Ikkaï &amp; Curtis (2008)</a>	14	21-35	Attentional cueing	Covert shift > Baseline	3T	Event-related	Y	ROIs	11	Y	Caret	MNI
<a href="#">Mao et al. (2007)</a>	12	24.3; 21-27	Spatial cueing	Attention to peripheral locations > Fixation	3T	Blocked	N	Whole-brain	6	N	SPM99	Talairach
<a href="#">Mohanty et al. (2009)</a>	13	27 ± 3.8	Spatial cueing / Visual search	Valid > Neutral trials	3T	Event-related	Y	Whole-brain	10	N	SPM5	MNI
<a href="#">Vossel et al. (2012)</a>	24	26.83; 20-37	Spatial cueing	Valid trials > Baseline	3T	Event-related	Y	Whole-brain	6	N	SPM8	MNI
<a href="#">Wen et al. (2012)</a>	12	20-28	Spatial cueing	Attend > Passive viewing blocks	3T	Blocked	N	ROIs	7	N	SPM2	MNI
<a href="#">Xuan et al. (2016)</a>	24	26.3; 18-49	Attentional network test	Valid > Invalid trials	3T	Event-related	N	Whole-brain	20	N	SPM8	MNI

## Supplementary references

Brown MRG, Vilis T, Everling S (2007) Frontoparietal activation with preparation for antisaccades. *J Neurophysiol* 98:1751–1762. <https://doi.org/10.1152/jn.00460.2007>

Cameron IGM, Coe BC, Watanabe M, et al (2009) Role of the basal ganglia in switching a planned response. *Eur J Neurosci* 29:2413–2425. <https://doi.org/10.1111/j.1460-9568.2009.06776.x>

Chica AB, Paz-Alonso PM, Valero-Cabré A, Bartolomeo P (2013) Neural bases of the interactions between spatial attention and conscious perception. *Cereb Cortex* 23:1269–1279. <https://doi.org/10.1093/cercor/bhs087>

Fan J, Mccandliss TBD, Fossella J, et al (2005) The activation of attentional networks. 26:471–479. <https://doi.org/10.1016/j.neuroimage.2005.02.004>

Ford KA, Goltz HC, Brown MRG, Everling S (2005) Neural processes associated with antisaccade task performance investigated with event-related fMRI. *J Neurophysiol* 94:429–440. <https://doi.org/10.1152/jn.00471.2004>

Ikkaï A, Curtis CE (2008) Cortical activity time locked to the shift and maintenance of spatial attention. *Cereb Cortex* 18:1384–1394. <https://doi.org/10.1093/cercor/bhm171>

Manoach DS, Thakkar KN, Cain MS, et al (2007) Neural activity is modulated by trial history: A functional magnetic resonance imaging study of the effects of a previous antisaccade. *J Neurosci* 27:1791–1798. <https://doi.org/10.1523/JNEUROSCI.3662-06.2007>

Mao L, Zhou B, Zhou W, Han S (2007) Neural correlates of covert orienting of visual spatial attention along vertical and horizontal dimensions. *Brain Res* 1136:142–153. <https://doi.org/10.1016/j.brainres.2006.12.031>

Mohanty A, Egner T, Monti JM, Mesulam MM (2009) Search for a threatening target triggers limbic guidance of spatial attention. *J Neurosci* 29:10563–10572. <https://doi.org/10.1523/JNEUROSCI.1170-09.2009>

Neggers SFW, van Diepen RM, Zandbelt BB, et al (2012) A functional and structural investigation of the human fronto-basal volitional saccade network. *PLoS One* 7:. <https://doi.org/10.1371/journal.pone.0029517>

Pierce JE, McDowell JE (2015) Modulation of cognitive control levels via manipulation of saccade trial-type probability assessed with event-related BOLD fMRI. *J Neurophysiol* 115:763–772.

<https://doi.org/10.1152/jn.00776.2015>

Pierce JE, McDowell JE (2017) Contextual effects on cognitive control and BOLD activation in single versus mixed saccade tasks. *Brain Cogn* 115:12–20. <https://doi.org/10.1016/j.bandc.2017.03.003>

Salvia E, Harvey M, Nazarian B, Grosbras MH (2020) Social perception drives eye-movement related brain activity: Evidence from pro- and anti-saccades to faces. *Neuropsychologia* 139:107360.

<https://doi.org/10.1016/j.neuropsychologia.2020.107360>

Vossel S, Weidner R, Driver J, et al (2012) Deconstructing the architecture of dorsal and ventral attention systems with dynamic causal modeling. *J Neurosci* 32:10637–10648.

<https://doi.org/10.1523/JNEUROSCI.0414-12.2012>

Wen X, Yao L, Liu Y, Ding M (2012) Causal interactions in attention networks predict behavioral performance.

*J Neurosci* 32:1284–1292. <https://doi.org/10.1523/JNEUROSCI.2817-11.2012>

Xuan B, Mackie MA, Spagna A, et al (2016) The activation of interactive attentional networks. *Neuroimage*

129:308–319. <https://doi.org/10.1016/j.neuroimage.2016.01.017>